

# On the Linear Speedup of the Push-Pull Method for Decentralized Optimization over Digraphs

Liyuan Liang<sup>\*</sup>Gan Luo<sup>\*</sup>Kun Yuan<sup>†</sup>

## Abstract

The linear speedup property is essential for demonstrating the advantage of distributed algorithms over their single-node counterparts. In this paper, we study the stochastic PUSH-PULL method, a widely adopted decentralized optimization algorithm over directed graphs (digraphs). Unlike methods that rely solely on row-stochastic or column-stochastic mixing matrices, PUSH-PULL avoids nonlinear correction and has shown superior empirical performance across a variety of settings. However, its theoretical analysis remains challenging, and the linear speedup property has not been generally established—revealing a significant gap between empirical success and limited theoretical understanding. To bridge this gap, we propose a novel analysis framework and prove that PUSH-PULL achieves linear speedup over arbitrary strongly connected digraphs. Our results provide the comprehensive theoretical understanding for stochastic PUSH-PULL, aligning its theory with empirical performance. Code: <https://github.com/pkumelon/PushPull>.

## 1 Introduction

Scaling machine learning tasks to large datasets and models necessitates efficient distributed computation across multiple nodes. In distributed optimization, a network of  $n$  nodes cooperates to solve

$$\min_{x \in \mathbb{R}^d} f(x) := \frac{1}{n} \sum_{i=1}^n f_i(x) \quad \text{where} \quad f_i(x) = \mathbb{E}_{\xi_i \sim \mathcal{D}_i}[F(x; \xi_i)]. \quad (1)$$

Here,  $\xi_i$  denotes a random data sample drawn from the local distribution  $\mathcal{D}_i$ , and  $f_i : \mathbb{R}^d \rightarrow \mathbb{R}$  is the local loss function, which may be nonconvex. During optimization, each node  $i$  can access its own local gradient  $\nabla F_i(x; \xi_i)$ , but must communicate to obtain gradient information from the other nodes. Data heterogeneity is typically present in (1), meaning the local distributions  $\{\mathcal{D}_i\}_{i=1}^n$  differ across nodes. Consequently, the loss functions  $f_i(x)$  and  $f_j(x)$  are generally not equal, *i.e.*,  $f_i(x) \neq f_j(x)$ .

---

<sup>\*</sup>Equal contribution. Liyuan Liang and Gan Luo are with School of Mathematics Science, Peking University ([lianyuangg@gmail.com](mailto:lianyuangg@gmail.com), [2200013522@stu.pku.edu.cn](mailto:2200013522@stu.pku.edu.cn)),

<sup>†</sup>Corresponding author. Kun Yuan is with Center for Machine Learning Research, Peking University ([kunyuan@pku.edu.cn](mailto:kunyuan@pku.edu.cn))

Parallel stochastic gradient descent (SGD) is a widely adopted approach in distributed optimization, where local gradients are globally averaged using either a central server [1] or Ring All-Reduce communication primitives [2]. However, such global synchronization incurs substantial bandwidth overhead and high latency as the number of nodes increases, thereby hurting the scalability of the optimization process. To address these limitations, decentralized SGD has recently been proposed to solve problem (1) without requiring global gradient aggregation. In this setting, each node independently maintains and updates its model by communicating only with immediate neighbors, significantly reducing communication overhead. Beyond efficiency, decentralized algorithms offer improved robustness to node and link failures, maintaining convergence as long as the underlying communication graph remains connected. In contrast, centralized SGD breaks down if the central server crashes.

In this paper, we consider a general decentralized setting where the network topology is modeled as a strongly connected *directed graph (digraph)*, which naturally encompasses undirected networks as a special case. Compared to undirected graphs, digraphs are particularly well-suited for ad hoc decentralized systems, such as heterogeneous robotic networks that operate under asynchronous, one-sided communication and random node activation. More recently, digraphs have shown great potential in distributed deep learning, where certain classes of directed networks exhibit both topological sparsity and strong algebraic connectivity. These properties make them especially attractive for the distributed training of large-scale models. Notable examples include the exponential graph [3], EquiTopo [4], and B-ary tree [5].

## 1.1 Decentralized algorithms over digraphs

In any connected network, the topology can be characterized by a mixing matrix. This matrix reflects how nodes are connected and is important for understanding how the network affects algorithm performance. For undirected networks, it is straightforward to construct symmetric and doubly stochastic mixing matrices. For directed networks, achieving a doubly stochastic matrix is generally infeasible. Consequently, mixing matrices in such cases are typically either column-stochastic [6, 7] or row-stochastic [8, 9], but not both.

Building on the connectivity pattern of the underlying network topology, decentralized optimization algorithms over directed graphs can be broadly categorized into three families in the literature. The first family relies on the PUSH-SUM technique [10, 11], which employs column-stochastic mixing matrices for all communications. Accordingly, we refer to this class as PUSH-ONLY algorithms in this paper. When exact gradients  $\nabla f_i$  are available, the well-known SUBGRADIENT-PUSH algorithm [12, 11] converges to the desired solution, albeit with relatively slow sublinear rates even under strong convexity. More advanced methods such as EXTRA-PUSH [13], DEXTRA [14], ADD-OPT [15], and PUSH-DIGING [7] improve convergence speed by mitigating the effects of data heterogeneity. Stochastic variants, including SGD-PUSH [16] and S-ADDOPT [17], extend these approaches to settings with stochastic gradients.

The second family consists of algorithms that use only row-stochastic matrices for communication, referred to as the PULL-ONLY setting. Just as PUSH-SUM underpins the design of PUSH-ONLY algorithms, the

PULL-DIAG gossip protocol [9] serves as the foundation for ROW-ONLY methods. Building on PULL-DIAG, reference [9] adapted the distributed gradient descent algorithm to the ROW-ONLY setting. Subsequently, [18, 19] extended gradient tracking techniques to this framework, while momentum-based PULL-ONLY gradient tracking methods were developed by [20, 21].

The third family comprises algorithms that alternate between row-stochastic and column-stochastic mixing matrices, commonly referred to as the PUSH-PULL method [22] or the AB method [23]. In this framework, a row-stochastic matrix is used to exchange model parameters, while a column-stochastic matrix is employed to share gradient information. As demonstrated in [23, 22, 24], the PUSH-PULL family typically achieves significantly faster convergence rates than algorithms relying solely on column- or row-stochastic matrices. [25] extended the PUSH-PULL method to stochastic optimization settings, while [5] improved its convergence rate on B-ary tree network topologies. Accelerated or constrained variant of the PUSH-PULL method have also been explored in [26, 27].

## 1.2 Linear speedup in iteration complexity

*Linear speedup* refers to the property of a distributed algorithm whereby the number of iterations required to reach an  $\epsilon$ -accurate solution decreases linearly with the number of nodes. For example, centralized SGD achieves an  $\epsilon$ -accurate solution in  $\mathcal{O}\left(\frac{1}{n\epsilon^2}\right)$  iterations, where  $n$  denotes the number of nodes. This scaling behavior demonstrates that centralized SGD achieves linear speedup with respect to the number of nodes. The linear speedup property is crucial for establishing the advantage of distributed algorithms over their single-node counterparts. Without this property, the practical utility of a distributed algorithm may be limited, as it would offer little benefit from using multiple computing nodes.

The linear speedup property of decentralized algorithms over undirected graphs is well established. The first such analysis for decentralized SGD was presented in [28], demonstrating that decentralized SGD can achieve the same asymptotic convergence rate as its centralized counterpart. Building on this foundation, a variety of advanced decentralized algorithms—such as Exact Diffusion/NIDS [29, 30] and Gradient Tracking methods [31, 32, 33]—are proven to achieve linear speedup [34, 29, 35]. In addition, [36] provides a linear speedup analysis for decentralized SGD under time-varying undirected network topologies.

Recent literature has increasingly focused on establishing the linear speedup property of decentralized algorithms over digraphs. For PUSH-ONLY algorithms that employ column-stochastic mixing matrices, linear speedup has been formally proven in [16, 37]. Moreover, a recent study [38] proposes methods that achieve the optimal iteration complexity in this setting. For PULL-ONLY algorithms that employ row-stochastic mixing matrices, convergence has been extensively studied under various settings [9, 18, 19, 20, 21]; however, these analyses do not establish the linear speedup property. The main challenge lies in the fact that using a row-stochastic matrix alone introduces a deviation in the descent direction from the globally averaged gradient. With a novel analysis framework addressing this issue, the linear speedup property of PULL-ONLY algorithms was established only recently in [39]. These results reveal the effectiveness of PUSH-ONLY and

PULL-ONLY algorithms over digraphs.

However, although PUSH-PULL algorithms typically achieve significantly better empirical performance than PUSH-ONLY and PULL-ONLY methods, their linear speedup property has not been generally established. Existing theoretical analyses of PUSH-PULL remain limited, primarily focusing on strongly convex loss functions in deterministic settings [23, 40, 22, 5]. In the nonconvex and stochastic setting, neither linear speedup nor even basic convergence guarantees have been formally established for PUSH-PULL. The most relevant theoretical result to date is presented in [5], which introduces a variant called B-ary Tree Push-Pull (BTPP). While BTPP is shown to achieve linear speedup, the result relies on the specialized B-ary tree topology, and the analysis does not generalize to general network topologies.

### 1.3 Motivation and main results

Building on the above discussion, the existing theoretical convergence analyses for PUSH-PULL methods remain rather limited, underscoring a clear discrepancy between the weak theoretical guarantees and their strong empirical performance. This gap gives rise to the following two open questions:

- Q1. What is the intrinsic difference between the PUSH-PULL method and the other two families, *i.e.*, PUSH-ONLY and PULL-ONLY? Why is the theoretical analysis of PUSH-PULL more challenging?
- Q2. Can PUSH-PULL achieve linear speedup over a broader class of network topologies—for instance, all strongly connected digraphs?

Addressing these two questions is crucial for establishing a theoretical foundation that supports the effectiveness of PUSH-PULL methods.

Regarding Question Q1, we demonstrate that both PUSH-ONLY and PULL-ONLY algorithms closely align with centralized SGD; specifically, after a careful numerical transformation, their variable updates closely resemble those of centralized SGD. This structural similarity explains why the linear speedup property can be readily established for PUSH-ONLY and PULL-ONLY methods. In contrast, PUSH-PULL is not designed to align with centralized SGD and consistently exhibits a non-vanishing deviation from the centralized trajectory. Consequently, the linear speedup analysis for PUSH-PULL is substantially more challenging and fundamentally distinct from that of PUSH-ONLY and PULL-ONLY algorithms.

For Question Q2, we establish a linear speedup convergence result for the PUSH-PULL method. To the best of our knowledge, this is the first such result for PUSH-PULL over all strongly connected digraphs under standard assumptions, whereas existing analyses of stochastic PUSH-PULL [5, 41] are restricted to tree-structured topologies. By introducing a novel analysis framework that addresses the misalignment between PUSH-PULL and centralized SGD, this paper bridges the gap between the convergence theory and the strong empirical performance of the PUSH-PULL method.

The remainder of the paper is organized as follows. Section 2 introduces necessary notations, assumptions, and measures. Section 3 reviews the PUSH-ONLY, PULL-ONLY, and PUSH-PULL methods, and offers insights into the derivation of linear speedup convergence. In Section 4, we present the key components of our analysis and state the main convergence theorem. Section 5 provides extensive numerical experiments that demonstrate the ability of the PUSH-PULL method to achieve linear speedup. Finally, Section 6 concludes the paper.

## 2 Notations, Assumptions and Measures

This section introduces notations, assumptions, and measures that will be used throughout the paper.

**Notations.** The directed network is denoted by  $\mathcal{G} = (\mathcal{N}, \mathcal{E})$ , where  $\mathcal{N} = \{1, 2, \dots, n\}$  is the set of nodes and  $\mathcal{E}$  is the set of directed edges. An edge  $(j, i) \in \mathcal{E}$  indicates that node  $j$  can send information to node  $i$ . A directed graph is said to be *strongly connected* if there exists a directed path from any node to every other node in the graph. We say that  $\mathcal{G} = (\mathcal{N}, \mathcal{E})$  is the underlying topology of the weight matrix  $A = [a_{ij}]$  if  $A$  is entrywise nonnegative and  $a_{ij} > 0$  if and only if  $(j, i) \in \mathcal{E}$ . Let  $\mathbf{1} \in \mathbb{R}^n$  denote the all-ones vector. Set  $[n]$  denotes  $\{1, 2, \dots, n\}$ . For a vector  $v$ ,  $\text{Diag}(v)$  denotes the diagonal matrix with  $v$  as its diagonal entries.

We use matrix  $A$  to denote the row-stochastic matrix (*i.e.*,  $A\mathbf{1} = \mathbf{1}$ ) and matrix  $B$  to denote the column-stochastic matrix (*i.e.*,  $B^\top \mathbf{1} = \mathbf{1}$ ). The Perron vectors [42] of matrices  $A$  and  $B$ , if they exist, are denoted by  $\pi_A$  and  $\pi_B$ , respectively. We introduce  $A_\infty := \mathbf{1}\pi_A^\top$  and  $B_\infty := \pi_B\mathbf{1}^\top$ . Additionally, we define  $n \times d$  matrices

$$\begin{aligned}\mathbf{x}^{(k)} &:= [(x_1^{(k)})^\top; (x_2^{(k)})^\top; \dots; (x_n^{(k)})^\top] \\ \mathbf{g}^{(k)} &:= [\nabla F_1(x_1^{(k)}; \xi_1^{(k)})^\top; \dots; \nabla F_n(x_n^{(k)}; \xi_n^{(k)})^\top] \\ \nabla f(\mathbf{x}^{(k)}) &:= [\nabla f_1(x_1^{(k)})^\top; \dots; \nabla f_n(x_n^{(k)})^\top]\end{aligned}$$

by stacking local variables, where the subscript denotes the node index and the superscript indicates the iteration index. We define the filtration  $\mathcal{F}_k$  as the collection of all information available up to  $\mathbf{x}^{(k)}$ , excluding the stochastic gradient evaluated at  $\mathbf{x}^{(k)}$ . The notation  $\mathbb{E}_k[\cdot]$  denotes the conditional expectation  $\mathbb{E}[\cdot \mid \mathcal{F}_k]$ . The notation  $\|\cdot\|$  denotes the  $\ell_2$  norm for vectors, while  $\|\cdot\|_F$  denotes the Frobenius norm for matrices. The induced  $\ell_2$  norm for matrices is denoted by  $\|\cdot\|_2$ , defined as  $\|A\|_2 := \max_{\|v\|=1} \|Av\|$ .

**Assumptions.** We first specify the underlying graphs  $(\mathcal{G}_A, \mathcal{G}_B)$  and the corresponding weight matrices  $(A, B)$  used in the stochastic PUSH-PULL method.

**Assumption 1** (COMMUNICATION GRAPH). *Graphs  $\mathcal{G}_A$  and  $\mathcal{G}_B$  are strongly connected.*

**Assumption 2** (WEIGHT MATRIX). *The weight matrix  $A$  is row-stochastic with underlying digraph  $\mathcal{G}_A$ , and the weight matrix  $B$  is column-stochastic with underlying digraph  $\mathcal{G}_B$ . Both  $A$  and  $B$  have positive trace.*

Assumptions 1 and 2 are standard in the analysis of the PUSH-PULL method [24, 40, 26]. In our paper, their primary role is to facilitate the derivation of Proposition 1. Strictly speaking, these assumptions could be replaced as long as Proposition 1 remains valid, without affecting the main convergence results.

**Proposition 1** (EXPONENTIAL DECAY). *For  $A$  and  $B$  satisfying Assumptions 1 and 2, there exist entrywise positive Perron vectors  $\pi_A, \pi_B \in \mathbb{R}^n$  such that*

$$\pi_A^\top A = \pi_A^\top, \quad B\pi_B = \pi_B, \quad \|\pi_A\|_1 = \|\pi_B\|_1 = 1, \quad \pi_A^\top \pi_B > 0.$$

*Besides, there exists constants  $p_A, p_B > 0$ ,  $\lambda_A, \lambda_B \in [0, 1)$  such that*

$$\|A^k - A_\infty\|_2 \leq p_A \lambda_A^k, \quad \|B^k - B_\infty\|_2 \leq p_B \lambda_B^k, \quad \forall k \geq 0.$$

*Proof.* The proof follows directly from the Perron-Frobenius theorem [42]. □

Finally, we state standard assumptions regarding the stochastic gradients and function smoothness.

**Assumption 3** (GRADIENT ORACLE). *There exists a constant  $\sigma \geq 0$  such that*

$$\mathbb{E}_k[\nabla F_i(x_i^{(k)}; \xi_i^{(k)})] = \nabla f_i(x_i^{(k)}) \quad \text{and} \quad \mathbb{E}_k[\|\nabla F_i(x_i^{(k)}; \xi_i^{(k)}) - \nabla f_i(x_i^{(k)})\|_F^2] \leq \sigma^2$$

*for any  $i \in [n]$  and  $k \geq 0$ .*

**Assumption 4** (SMOOTHNESS). *There exist positive constants  $L, \Delta$  such that*

$$\|\nabla f_i(x) - \nabla f_i(y)\| \leq L\|x - y\| \quad \text{and} \quad f_i(x) - \inf_x f_i(x) \leq \Delta, \quad \forall i \in [n].$$

**Measures.** Various effective metrics have been proposed to capture the impact of digraphs on decentralized stochastic optimization. Let  $\Pi_A := \text{Diag}(\pi_A)$  and  $\Pi_B := \text{Diag}(\pi_B)$ . Given a column-stochastic mixing matrix  $B$ , references [25, 38] introduce  $\beta_B := \|\Pi_B^{1/2}(B - B_\infty)\Pi_B^{-1/2}\|_2 \in [0, 1)$  as a measure of graph connectivity, and define  $\kappa_B := \max \pi_B / \min \pi_B$  to reflect the deviation of the equilibrium distribution  $\pi_B$  from the uniform distribution  $n^{-1}\mathbf{1}$ . Similarly, reference [38] introduces  $\beta_A := \|\Pi_A^{1/2}(A - A_\infty)\Pi_A^{-1/2}\|_2 \in [0, 1)$  and  $\kappa_A := \max \pi_A / \min \pi_A$  to characterize the influence of the row-stochastic mixing matrix  $A$  on decentralized algorithms.

However, this paper introduces a new set of metrics to facilitate the convergence analysis of the PUSH-PULL method. When Proposition 1 holds, we define the following constants:

$$s_A := \max\left\{\sum_{i=0}^{\infty} \|A^i - A_\infty\|_2, \sum_{i=0}^{\infty} \|A^i - A_\infty\|_2^2\right\}, \tag{2}$$

$$s_B := \max\left\{\sum_{i=0}^{\infty} \|B^i - B_\infty\|_2, \sum_{i=0}^{\infty} \|B^i - B_\infty\|_2^2\right\}, \tag{3}$$

$$c := n \pi_A^\top \pi_B. \tag{4}$$

Throughout this paper, we characterize the influence of the mixing matrices using only  $s_A$ ,  $s_B$ ,  $c$ , and  $n$ . A connection between these quantities and the previously discussed metrics is established in Proposition 2.

**Proposition 2** (RELATION WITH OTHER MEASURES). *Suppose Assumption 1 and 2 hold. The following inequalities on  $s_A$ ,  $s_B$  and  $c$  hold:*

$$1 \leq s_A \leq \frac{M_A^2(1 + \frac{1}{2} \ln(\kappa_A))}{1 - \beta_A}, \quad 1 \leq s_B \leq \frac{M_B^2(1 + \frac{1}{2} \ln(\kappa_B))}{1 - \beta_B},$$

$$n \max\{\min \pi_A, \min \pi_B\} \leq c \leq n \min\{\max \pi_A, \max \pi_B\}.$$

where  $M_A := \max_{i \geq 0} \|A^i - A_\infty\|_2$ ,  $M_B := \max_{i \geq 0} \|B^i - B_\infty\|_2$ .

*Proof.* See Appendix A. □

### 3 Preliminary

In this section, we present a concise overview of the linear speedup analysis for the PUSH-ONLY and PULL-ONLY algorithms. We also discuss the limitations of existing analytical approaches and explain why they cannot be directly extended to the PUSH-PULL algorithm.

#### 3.1 Push-Only and Pull-Only methods align with centralized SGD

Most decentralized algorithms—such as decentralized SGD [36], gradient tracking [31, 32, 43, 44], gradient-Push [45], Push-DiGing [7], gradient-Pull [9], and FROST [19]—are designed to emulate centralized SGD in a decentralized setting. These algorithms can generally be transformed into the following form:

$$\hat{x}^{(k+1)} = \hat{x}^{(k)} - \alpha \bar{g}^{(k)} + \epsilon^{(k)} \quad (5)$$

where  $\hat{x}^{(k)} = \sum_{i=1}^n v_i^{(k)} (x_i^{(k)})^\top \in \mathbb{R}^{1 \times d}$  is a convex combination of the local optimization variables, with  $v_i^{(k)}$  denoting the combination weights, and  $\bar{g}^{(k)} = \frac{1}{n} \mathbf{1}^\top \mathbf{g}^{(k)}$  is the average stochastic gradient. The term  $\epsilon^{(k)}$  captures additional error due to the decentralized nature of the algorithm.

For PUSH-ONLY and PULL-ONLY optimization algorithms, the additional error term  $\epsilon$  is carefully designed to be either zero or to decay exponentially fast. This design ensures that the trajectories of the local decision variables closely track those of centralized SGD. When the error is sufficiently small, the linear speedup result naturally follows from the same analytical framework used for centralized SGD. Below, we provide a brief example illustrating how to derive the formulation in (5).

**Example 1** (PUSH-DIGING [7]). *The Push-Diging algorithm iterates as follows:*

$$\mathbf{x}^{(k+1)} = A_k \mathbf{x}^{(k)} - \alpha V_{k+1}^{-1} \mathbf{y}^{(k)}, \quad (6a)$$

$$\mathbf{y}^{(k+1)} = B \mathbf{y}^{(k)} + \mathbf{g}^{(k+1)} - \mathbf{g}^{(k)}, \quad (6b)$$

where  $v_k = B^k \mathbf{1}$ ,  $V_k = \text{Diag}(v_k)$  is a diagonal matrix,  $A_k = V_{k+1}^{-1} B V_k$ , and  $\mathbf{g}^{(k)}$  is the stacked stochastic gradient defined in the notation section. By left-multiplying both sides of (6a) by  $n^{-1} v_{k+1}^\top$ , we obtain

$$n^{-1} v_{k+1}^\top \mathbf{x}^{(k+1)} = n^{-1} v_k^\top \mathbf{x}^{(k)} - \alpha \bar{g}^{(k)}.$$

Letting  $\hat{x}^{(k)} = n^{-1}v_k^\top \mathbf{x}^{(k)}$ , this update exactly matches the form in (5).

**Example 2** (FROST [18, 19]). FROST/PullDiag-GT algorithm only relies on a row-stochastic matrix  $A$ .

Its recursion can be written as follows:

$$\mathbf{x}^{(k+1)} = A\mathbf{x}^{(k)} - \alpha\mathbf{y}^{(k)}, \quad (7a)$$

$$\mathbf{y}^{(k+1)} = A\mathbf{y}^{(k)} + D_{k+1}^{-1}\mathbf{g}^{(k+1)} - D_k^{-1}\mathbf{g}^{(k)}, \quad (7b)$$

where  $D_k = \text{Diag}(A^k)$  is a diagonal matrix,  $\mathbf{g}^{(k)}$  is the stacked stochastic gradient and  $\mathbf{y}^{(0)} = \mathbf{g}^{(0)}$ . By left-multiplying both sides of (7a) by  $n^{-1}\pi_A^\top$ , we obtain

$$n^{-1}\pi_A^\top \mathbf{x}^{(k+1)} = n^{-1}\pi_A^\top \mathbf{x}^{(k)} - \alpha\bar{g}^{(k)} + \epsilon^{(k)},$$

where  $\epsilon^{(k)} = \alpha n^{-1}(\mathbf{1}^\top - \pi_A^\top D_k^{-1})\mathbf{g}^{(k)}$  converges to zero exponentially fast [Lemma 12, [39]]. Letting  $\hat{x}^{(k)} = n^{-1}\pi_A^\top \mathbf{x}^{(k)}$ , this update matches the form (5).

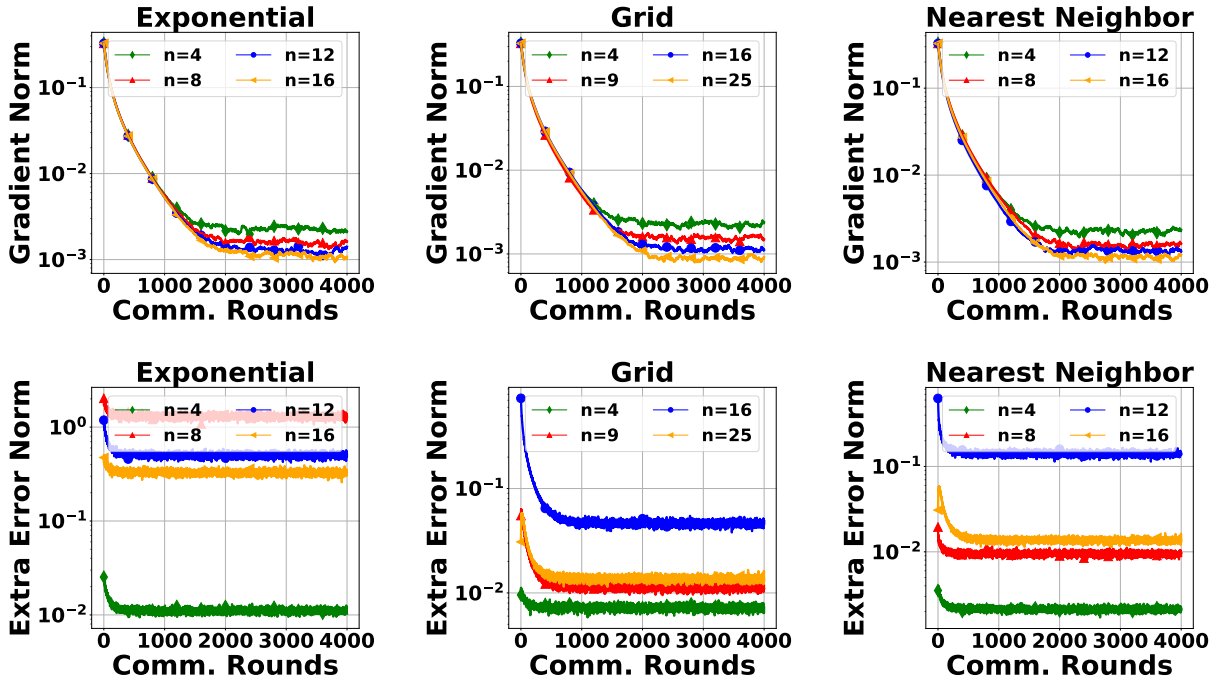


Figure 1: The extra error does not vanish. The top three plots illustrate the convergence behavior across different network topologies, while the bottom three plots demonstrate that the size of extra error term rapidly stabilizes and persists as a significant constant. The experiment is a logistic regression on synthetic dataset. We use stochastic gradients and a constant learning rate 0.005, and detailed settings is referred to Appendix C.



### 3.2 PUSH-PULL suffers from extra error terms

Unlike the aforementioned algorithms, it is generally impossible to reformulate PUSH-PULL to obtain a centralized SGD-like update. The recursion of PUSH-PULL is

$$\mathbf{x}^{(k+1)} = A\mathbf{x}^{(k)} - \alpha\mathbf{y}^{(k)}, \quad (8a)$$

$$\mathbf{y}^{(k+1)} = B\mathbf{y}^{(k)} + \mathbf{g}^{(k+1)} - \mathbf{g}^{(k)}, \quad (8b)$$

where  $A, B$  are row-stochastic and column-stochastic matrices determined by the topology,  $x_1^{(0)} = x_2^{(0)} = \dots = x_n^{(0)} = x^{(0)}$ ,  $\mathbf{y}^{(0)} = \mathbf{g}^{(0)}$ . Left-multiplying both sides of (8b) by  $\mathbf{1}^\top$ , we achieve

$$\mathbf{1}^\top \mathbf{y}^{(k+1)} = \mathbf{1}^\top \mathbf{y}^{(k)} + \mathbf{1}^\top \mathbf{g}^{(k+1)} - \mathbf{1}^\top \mathbf{g}^{(k)} = \mathbf{1}^\top \mathbf{g}^{(k+1)}, \quad (9)$$

where the last equality holds due to the initialization  $\mathbf{y}^{(0)} = \mathbf{g}^{(0)}$ . Next, we left-multiply both sides of (8a) by  $\pi_A^\top$ , which yields

$$\begin{aligned} \pi_A^\top \mathbf{x}^{(k+1)} &= \pi_A^\top A\mathbf{x}^{(k)} - \alpha\pi_A^\top B\mathbf{y}^{(k)} - \alpha\pi_A^\top (I - B_\infty)\mathbf{y}^{(k)} \\ &= \pi_A^\top \mathbf{x}^{(k)} - \alpha\pi_A^\top \pi_B \mathbf{1}^\top \mathbf{y}^{(k)} - \alpha\pi_A^\top (I - B_\infty)\mathbf{y}^{(k)}. \end{aligned}$$

Let  $\hat{x}^{(k)} = \pi_A^\top \mathbf{x}^{(k)}$ , and recall from (9) that  $\mathbf{1}^\top \mathbf{y}^{(k)} = \mathbf{1}^\top \mathbf{g}^{(k)}$ . Then, we have

$$\hat{x}^{(k+1)} = \hat{x}^{(k)} - c\alpha\bar{g}^{(k)} - \alpha\pi_A^\top (I - B_\infty)\mathbf{y}^{(k)}, \quad (10)$$

where  $c = n\pi_A^\top \pi_B$  is a constant and  $\bar{g}^{(k)} = n^{-1}\mathbf{1}^\top \mathbf{g}^{(k)}$ . We observe that the error term  $\pi_A^\top (I - B_\infty)\mathbf{y}^{(k)}$  does not vanish but remains a large constant, see Figure 1.

This non-vanishing error term makes achieving linear speedup in PUSH-PULL highly nontrivial, because in traditional linear speedup analysis, only the noise from  $\|\bar{g}^{(k)}\|^2$  is the dominating factor. But here, both the squared error term  $\|\pi_A^\top (I - B_\infty)\mathbf{y}^{(k)}\|^2$  and the cross product  $\langle \bar{g}^{(k)}, \pi_A^\top (I - B_\infty)\mathbf{y}^{(k)} \rangle$  can introduce additional noise that may dominate the noise in  $\bar{g}^{(k)}$ .

For certain specific topologies, the error term can be ignored or absorbed. For instance, the work in [5] explores a special case known as the  $B$ -ary tree PUSH-PULL (BTPP) and demonstrates the linear speedup result on this particular topology. In BTPP,  $\pi_A = \pi_B = [1, 0, \dots, 0]^\top$ , leading to  $\pi_A^\top (I - B_\infty) = (0, -1, -1, \dots, -1)$ . By setting the loss function at the first node to zero,  $\pi_A^\top (I - B_\infty)\mathbf{y}^{(k)} = -n\bar{g}^{(k)}$  is achieved, which simplifies the process of achieving linear speedup. Another case is when  $A$  is doubly-stochastic; we have  $\pi_A^\top (I - B_\infty) = 0$ , which removes the error term.

Unfortunately, for general topologies, the error term lacks exploitable structure. This usually leads to a significant overestimation of the noise term, which in turn obstructs the derivation of a linear speedup result. Therefore, we recognize the central challenge in the analysis of stochastic Push-Pull: *How to estimate the noise level in error terms more accurately?* We tackle this key question in the following section.

## 4 Achieving Linear Speedup for Push-Pull

For simplicity, we denote  $\Delta_y^{(k)} := (I - B_\infty)\mathbf{y}^{(k)}$ . Using the gradient tracking recursion (8b), we discover the following relationship about extra error terms: for any integer  $k \geq 0, m \geq 1$ :

$$\sum_{i=0}^{m-1} \Delta_y^{(k+i)} = \left( \sum_{j=0}^{m-1} (B^j - B_\infty) \right) \Delta_y^{(k)} + \sum_{j=1}^{m-1} (B^{m-j-1} - B_\infty) (\mathbf{g}^{(k+j)} - \mathbf{g}^{(k)}). \quad (11)$$

To understand this equation, we propose the following important supporting lemma:

**Lemma 3.** *For any  $l \geq 0$  and any matrices  $M^{(0)}, M^{(1)}, \dots, M^{(l)} \in \mathbb{R}^{n \times n}$ . For any  $k \geq 0$ , If  $H = \sum_{i=0}^l M^{(i)} \mathbf{g}^{(k+i)}$  is a linear combination of stochastic gradients, then*

$$\mathbb{E}_k[\|H\|_F^2] \leq n\sigma^2 \sum_{i=0}^l \|M^{(i)}\|_2^2 + \mathbb{E}_k[\|\sum_{i=0}^l M^{(i)} \nabla f(\mathbf{x}^{(k+i)})\|_F^2].$$

*Proof.* This is a natural corollary of Assumption 3.  $\square$

Now we turn to the noise estimation for  $\mathbb{E}_k[\|\sum_{i=0}^{m-1} \Delta_y^{(k+i)}\|_F^2]$ . A common analysis using Cauchy's inequality typically provides

$$\mathbb{E}_k[\|\sum_{i=0}^{m-1} \Delta_y^{(k+i)}\|_F^2] \leq m \sum_{i=0}^{m-1} \mathbb{E}_k[\|\Delta_y^{(k+i)}\|_F^2] \lesssim m^2 \sigma^2. \quad (12)$$

Here, we use  $\lesssim$  to absorb matrix-related constants and focus on  $\sigma^2$ -related terms. Nevertheless, analysis using Equation (11) and Lemma 3 can be significantly better. Proposition 2 ensures that  $\sum_{j=1}^{m-1} \|B^{m-j-1} - B_\infty\|_2^2 + \|\sum_{j=1}^{m-1} B^{m-j-1} - B_\infty\|_2^2$  is finite. Therefore, applying Lemma 3 to Equation (11) tells us

$$\begin{aligned} \mathbb{E}_k[\|\sum_{i=0}^{m-1} \Delta_y^{(k+i)}\|_F^2] &\lesssim \mathbb{E}_k[\|\Delta_y^{(k)}\|_F^2] + \sigma^2 \\ &+ \mathbb{E}_k[\|\sum_{j=1}^{m-1} (B^{m-j-1} - B_\infty)(\nabla f(\mathbf{x}^{(k+j)}) - \nabla f(\mathbf{x}^{(k)}))\|_F^2] \\ &\lesssim \sigma^2 + \alpha^2 L^2 m^2 \sigma^2. \end{aligned} \quad (13)$$

Estimate from (13) sufficiently exploits the structure of gradient tracking, thus exhibiting  $\mathcal{O}(m^2)$  improvement compared to a naive estimate (12). To effectively leverage the result of (13), we introduce an  $m$ -step descent lemma. It comes from applying the standard descent lemma to the following recursion:

$$\hat{x}^{(k+m)} = \hat{x}^{(k)} - c\alpha \sum_{i=0}^{m-1} \bar{g}^{(k+i)} - \alpha \pi_A^\top \sum_{i=0}^{m-1} \Delta_y^{(k+i)}. \quad (14)$$

**Lemma 4** (M-STEP DESCENT LEMMA). *Suppose Assumption 3, 4 and Proposition 1 hold. For any integers  $k \geq 0$ , we define  $\hat{x}^{(k)} = \pi_A^\top \mathbf{x}^{(k)}$ . When  $\alpha \leq \frac{1}{6cmL}$ , the following inequality holds for any integers  $k \geq 0, m \geq$*

$6c^{-2}s_B^2$ :

$$\begin{aligned}
& \frac{\alpha cm}{4} \|\nabla f(\hat{x}^{(k)})\|^2 + \frac{\alpha c}{4} \sum_{i=0}^{m-1} \mathbb{E}_k[\|\overline{\nabla f}^{(k+i)}\|^2] \\
& \leq f(\hat{x}^{(k)}) - \mathbb{E}_k[f(\hat{x}^{(k+m)})] + \frac{2\alpha^2 c^2 mL}{n} \sigma^2 + 2\alpha^2 L n s_B^2 \sigma^2 \\
& \quad + \frac{c\alpha L^2}{2} \Delta_1^{(k)} + \frac{c\alpha L^2}{2} \Delta_2^{(k)} + \frac{3\alpha s_B^2}{cm} \|\Delta_y^{(k)}\|_F^2,
\end{aligned} \tag{15}$$

where

$$\Delta_1^{(k)} = \sum_{i=0}^{m-1} \mathbb{E}_k[\|\mathbf{x}^{(k+i)} - \hat{\mathbf{x}}^{(k)}\|_F^2], \quad \Delta_2^{(k)} = \sum_{j=1}^m \mathbb{E}_k[\|\mathbf{x}^{(k+j)} - \mathbf{x}^{(k)}\|_F^2].$$

The remaining errors are estimated in the next lemma.

**Lemma 5** (REMAINING ERRORS). *Suppose Assumption 3, 4 and Proposition 1 hold. With  $\Delta_1^{(k)}, \Delta_2^{(k)}$  defined above, when  $\alpha \leq \min\{\frac{1}{10cm\sqrt{s_B s_{B^m}^2} L}, \frac{1}{6L}\}$  and  $m \geq C_m$ , we have*

$$\begin{aligned}
& \frac{c\alpha L^2}{2} \sum_{k \in [m^*]} \mathbb{E}[\Delta_1^{(k)} + \Delta_2^{(k)}] + \frac{3\alpha s_B^2}{cm} \sum_{k \in [m^*]} \mathbb{E}[\|\Delta_y^{(k)}\|_F^2] \\
& \leq \frac{\alpha c}{4} \sum_{t=0}^{mK-1} \mathbb{E}_k[\|\overline{\nabla f}^{(t)}\|^2] + \frac{\alpha cm}{4} \left( \frac{73c\alpha L}{n} + \frac{384s_B^3 s_{B^m}^2}{m^2 c^2} \right) \sigma^2 + C_{\Delta,1} \frac{c\alpha L \Delta}{4m}.
\end{aligned}$$

where we define  $[m^*] := \{0, m, \dots, (K-1)m\}$ , and  $C_m$  and  $C_{\Delta,1}$  are matrix-related constants.  $s_{B^m}$  is the measure defined for  $B^m$ , see (3). Generally, we have  $s_{B^m} \leq s_B$ , and  $s_{B^m}$  converges to  $\|I - B_\infty\|_2$  for large  $m$ .

We are ready to state the main result of this paper.

**Theorem 1.** *Suppose Assumption 3, 4 and Proposition 1 hold. For given positive integers  $m$  and  $K$ , we define  $T := mK$ . When  $\alpha \leq \frac{1}{10cm\sqrt{s_B s_{B^m}^2} L}$  and  $m \geq C_m$ , we have*

$$\frac{1}{K} \sum_{k \in [m^*]} \mathbb{E}[\|\nabla f(\hat{x}^{(k)})\|^2] \leq \frac{4\Delta}{c\alpha T} + \frac{100c\alpha L}{n} \sigma^2 + \frac{384s_B^3 s_{B^m}^2}{m^2 c^2} \sigma^2 + C_{\Delta,1} \frac{L\Delta}{mT}. \tag{16}$$

where  $C_m$  and  $C_{\Delta,1}$  are matrix-related constants. Furthermore, if we choose

$$\begin{aligned}
m &= \lceil \max\{4c^{-1} s_B^{1.5} s_{B^m} \left( \frac{nT\sigma^2}{L\Delta} \right)^{0.25}, C_m\} \rceil, \\
\alpha &= \min \left\{ \frac{\sqrt{n\Delta}\sigma}{10c\sqrt{LT}}, \frac{1}{10cm\sqrt{s_B s_{B^m}^2} L}, \frac{1}{6L} \right\},
\end{aligned}$$

we reach that

$$\begin{aligned}
\min_{t \in \{0,1,\dots,T-1\}} \mathbb{E}[\|\nabla f(\hat{x}^{(t)})\|^2] & \leq \frac{44\sigma\sqrt{L\Delta}}{\sqrt{nT}} + \frac{L\Delta(m^{-1}C_{\Delta,1} + 10m\sqrt{s_B s_{B^m}^2} + c^{-1})}{T} \\
& = \frac{44\sigma\sqrt{L\Delta}}{\sqrt{nT}} + \mathcal{O}\left(\frac{L\Delta}{T}\right)^{\frac{3}{4}} + \mathcal{O}\left(\frac{L\Delta}{T}\right).
\end{aligned} \tag{17}$$

*Proof.* See Appendix B.3 □

**Comparison with existing analyses.** Theorem 1 provides the first finite-time non-convex convergence result for stochastic PUSH-PULL, while previous analyses focus either on the strongly convex case [46, 40] or on variants of PUSH-PULL relying on specific topologies [5]. The first term  $\frac{44\sigma\sqrt{L\Delta}}{\sqrt{nT}}$  explicitly shows that PUSH-PULL enjoys a linear speedup on arbitrary topologies satisfying Proposition 2.

**Impact of  $m$ :** In our analysis, we consider  $m$ -step gradient descent. The parameter  $m$  effectively controls the terms related to  $\sigma^2$  from additional errors, as illustrated by the  $\mathcal{O}(m^{-2}\sigma^2)$  term in (16).  $m$  cannot be arbitrarily large because larger values of  $m$  restrict the range of the learning rate, resulting in slower convergence and longer transient times in the analysis. In summary, the parameter  $m$  allows for a tradeoff between noise level and transient time.

**Transient time.** Our theorem is able to provide a coarse estimate for the transient time, which is

$$\max\{n^2c^{-4}s_B^8, n^7c^{-4}s_A^2s_B^3, nc^{-4}s_B^4\}.$$

The order of  $n$  is overestimated because we frequently use  $\|\pi_A\| \leq 1$  and  $\|\pi_B\| \leq 1$ , leading to a loss of  $n$  when  $A$  or  $B$  is doubly-stochastic.

## 5 Experiment

In this section, we empirically investigate the linear speedup properties of the PUSH-PULL algorithm across diverse network topologies. For the stochastic gradient oracle, we ensure that each node operates on a local dataset, computing gradients from randomly sampled data points at each iteration. The experimental validation proceeds in two phases: first, we examine a nonconvex regression problem using synthetic data, followed by training a fully connected neural network on the heterogeneously distributed MNIST dataset.

To further assess practical performance on established benchmarks, we extend our evaluation to ResNet-18 training on CIFAR-10. The distributed training experiments are conducted across multiple nodes ( $n > 1$ ) using three distinct network topologies: directed exponential graphs, grid graphs, and undirected random graphs. All results are systematically compared against the single-node baseline ( $n = 1$ ) to quantify the speedup achieved through distributed optimization.

Complete implementation specifications are provided in Appendix C. The source code and experimental scripts are publicly available in [our GitHub repository](#).

### 5.1 Nonconvex Logistic Regression on Synthetic Dataset

In the first experiment, the loss function at each node is a logistic regression function with nonconvex regularization terms (see (44) in Appendix C). We studied six different network topologies: the exponential,

grid, and ring graphs are directed, while the random, geometric, and nearest neighbor graphs are undirected. The mixing matrices  $A$  and  $B$  are generated by a special procedure (see Appendix C.1), which produces row-stochastic or column-stochastic matrices, but not doubly-stochastic ones.

We can observe clear linear speedup curves in Figure 2. For each topology, the noise level in gradients decreases proportionally to the square root of the number of nodes after the same number of communication rounds. All learning rates are set to  $lr = 0.005$ .

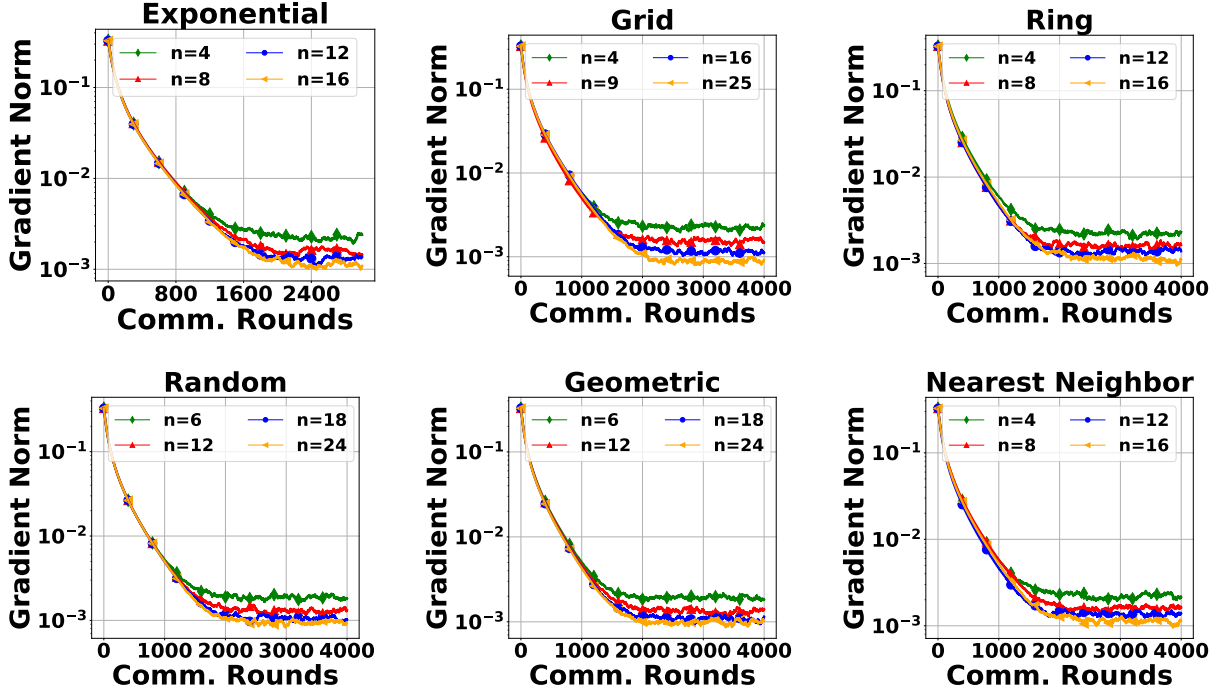


Figure 2: Linear speedup performance over various topologies on synthetic data, the learning rates are all 0.005.

## 5.2 Training Neural Network for MNIST Classification

In the second experiment, we trained a three-layer fully connected neural network for MNIST classification. We used the same topologies as before: directed exponential, grid, and ring graphs, and undirected random, geometric, and nearest neighbor graphs. Data is distributed heterogeneously using a Directlet distribution, see Appendix C.3. Figure 3 shows that PUSH-PULL is able to achieve linear speedup on both directed and undirected topologies.

## 5.3 Training Neural Network for CIFAR10 Image Classification

In the third experiment, we trained Resnet18 for CIFAR10 classification across different numbers of nodes and various topologies. We used three topologies mentioned before: directed exponential, grid graphs, and undirected random graphs. Here  $n = 1$  means training a single Resnet18 on a single-node without distributed

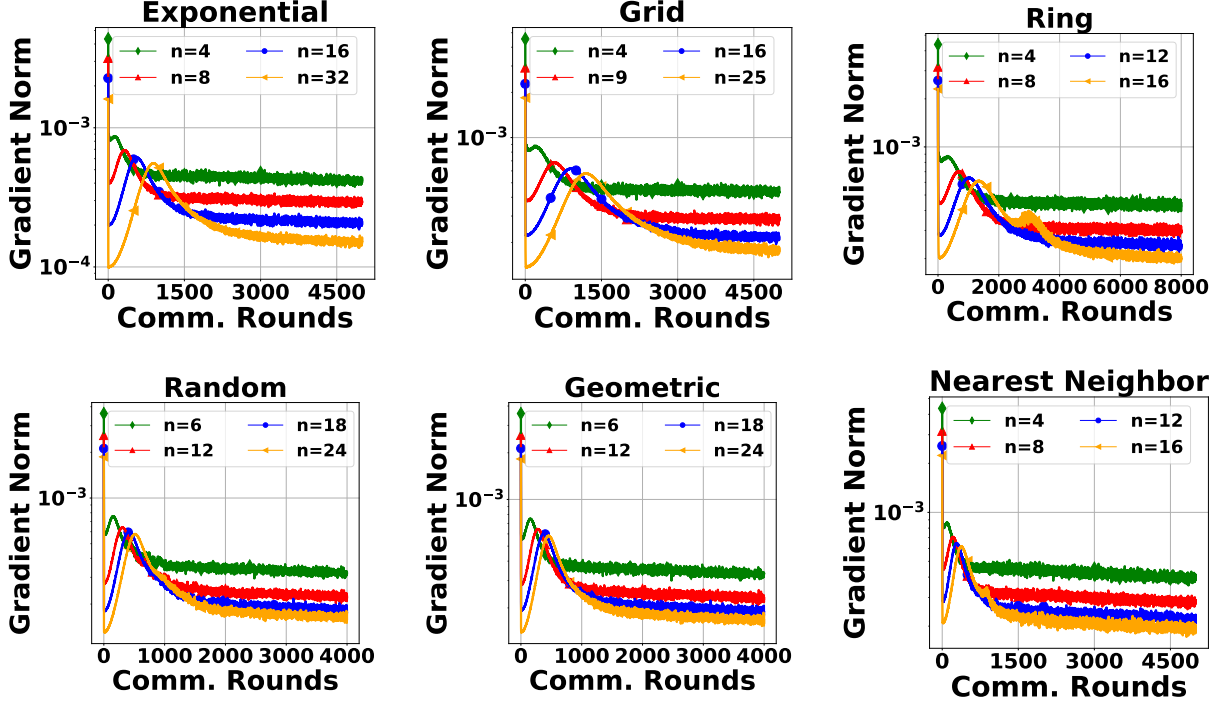


Figure 3: Linear speedup performance over various topologies, the learning rates are the same over the same topology.

optimization.

Figure 4 demonstrates the performance of our PUSH-PULL method. We observe that PUSH-PULL’s accuracy is initially lower compared to single-node optimization, which can be attributed to the overhead of the influence of topology. Nevertheless, after a sufficient number of epochs, PUSH-PULL achieves superior accuracy, leveraging its inherent speed advantages.

## 6 Conclusion

In this paper, we introduce a novel analysis technique and demonstrate linear speedup convergence for the PUSH-PULL method across arbitrary strongly connected topologies. This discovery enhances the community’s comprehension of the PUSH-PULL method and validates its effectiveness. Numerical experiments have corroborated our theoretical findings.

## References

- [1] Mu Li, David G Andersen, Jun Woo Park, Alexander J Smola, Amr Ahmed, Vanja Josifovski, James Long, Eugene J Shekita, and Bor-Yiing Su. Scaling distributed machine learning with the parameter server. In *11th USENIX Symposium on Operating Systems Design and Implementation (OSDI 14)*, pages 583–598, 2014.

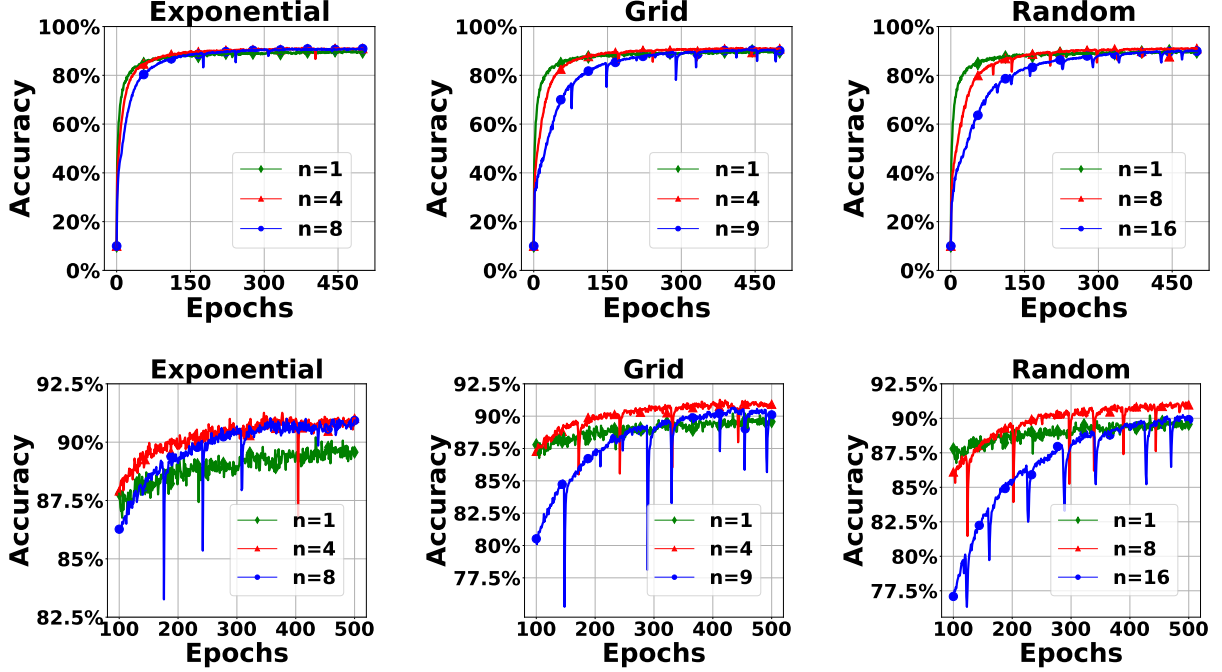


Figure 4: The test accuracy across different numbers of nodes and various topologies. All experiments were conducted using a learning rate of 0.005. The lower three figures specifically depict the accuracy after 100 epochs.

- [2] Pitch Patarasuk and Xin Yuan. Bandwidth optimal all-reduce algorithms for clusters of workstations. *Journal of Parallel and Distributed Computing*, 69(2):117–124, 2009.
- [3] Bicheng Ying, Kun Yuan, Yiming Chen, Hanbin Hu, Pan Pan, and Wotao Yin. Exponential graph is provably efficient for decentralized deep training. *Advances in Neural Information Processing Systems*, 34:13975–13987, 2021.
- [4] Zhuoqing Song, Weijian Li, Kexin Jin, Lei Shi, Ming Yan, Wotao Yin, and Kun Yuan. Communication-efficient topologies for decentralized learning with  $o(1)$  consensus rate. *Advances in Neural Information Processing Systems*, 35:1073–1085, 2022.
- [5] Runze You and Shi Pu. B-ary tree push-pull method is provably efficient for decentralized learning on heterogeneous data, 2024.
- [6] Angelia Nedić and Alex Olshevsky. Distributed optimization over time-varying directed graphs. *IEEE Transactions on Automatic Control*, 60(3):601–615, 2014.
- [7] Angelia Nedić, Alex Olshevsky, and Wei Shi. Achieving geometric convergence for distributed optimization over time-varying graphs. *SIAM Journal on Optimization*, 27(4):2597–2633, 2017.
- [8] Ali H Sayed. Adaptive networks. *Proceedings of the IEEE*, 102(4):460–497, 2014.

- [9] Van Sy Mai and Eyad H Abed. Distributed optimization over weighted directed graphs using row stochastic matrix. In *2016 American Control Conference (ACC)*, pages 7165–7170. IEEE, 2016.
- [10] David Kempe, Alin Dobra, and Johannes Gehrke. Gossip-based computation of aggregate information. In *44th Annual IEEE Symposium on Foundations of Computer Science, 2003. Proceedings.*, pages 482–491. IEEE, 2003.
- [11] Konstantinos I Tsianos, Sean Lawlor, and Michael G Rabbat. Push-sum distributed dual averaging for convex optimization. In *2012 IEEE 51st IEEE conference on decision and control (cdc)*, pages 5453–5458. IEEE, 2012.
- [12] Angelia Nedić and Alex Olshevsky. Distributed optimization over time-varying directed graphs. *IEEE Transactions on Automatic Control*, 60(3):601–615, 2015.
- [13] Jinshan Zeng and Wotao Yin. Extrapush for convex smooth decentralized optimization over directed networks. *Journal of Computational Mathematics*, pages 383–396, 2017.
- [14] Chenguang Xi and Usman A Khan. Dextra: A fast algorithm for optimization over directed graphs. *IEEE Transactions on Automatic Control*, 62(10):4980–4993, 2017.
- [15] Chenguang Xi, Ran Xin, and Usman A Khan. Add-opt: Accelerated distributed directed optimization. *IEEE Transactions on Automatic Control*, 63(5):1329–1339, 2017.
- [16] Mahmoud Assran, Nicolas Loizou, Nicolas Ballas, and Mike Rabbat. Stochastic gradient push for distributed deep learning. In *International Conference on Machine Learning*, pages 344–353. PMLR, 2019.
- [17] Muhammad I Qureshi, Ran Xin, Soumya Kar, and Usman A Khan. S-addopt: Decentralized stochastic first-order optimization over directed graphs. *IEEE Control Systems Letters*, 5(3):953–958, 2020.
- [18] Huaqing Li, Jinneng Wang, and Zheng Wang. Row-stochastic matrices based distributed optimization algorithm with uncoordinated step-sizes. In *2019 6th International Conference on Information, Cybernetics, and Computational Social Systems (ICCSS)*, pages 124–131. IEEE, 2019.
- [19] Ran Xin, Chenguang xi, and Usman Khan. Frost—fast row-stochastic optimization with uncoordinated step-sizes. *EURASIP Journal on Advances in Signal Processing*, 2019, 01 2019.
- [20] Diyako Ghaderyan, Necdet Serhat Aybat, A Pedro Aguiar, and Fernando Lobo Pereira. A fast row-stochastic decentralized method for distributed optimization over directed graphs. *IEEE Transactions on Automatic Control*, 69(1):275–289, 2023.
- [21] Qingguo Lü, Xiaofeng Liao, Huaqing Li, and Tingwen Huang. A nesterov-like gradient tracking algorithm for distributed optimization over directed networks. *IEEE Transactions on Systems, Man, and Cybernetics: Systems*, 51(10):6258–6270, 2020.



- [22] Shi Pu, Wei Shi, Jinming Xu, and Angelia Nedić. Push–pull gradient methods for distributed optimization in networks. *IEEE Transactions on Automatic Control*, 66(1):1–16, 2020.
- [23] Ran Xin and Usman A Khan. A linear algorithm for optimization over directed graphs with geometric convergence. *IEEE Control Systems Letters*, 2(3):315–320, 2018.
- [24] Angelia Nedić, Duong Thuy Anh Nguyen, and Duong Tung Nguyen. Ab/push-pull method for distributed optimization in time-varying directed networks. *Optimization Methods and Software*, pages 1–28, 2023.
- [25] Ran Xin, Anit Kumar Sahu, Usman A Khan, and Soumya Kar. Distributed stochastic optimization with gradient tracking over strongly-connected networks. In *2019 IEEE 58th Conference on Decision and Control (CDC)*, pages 8353–8358. IEEE, 2019.
- [26] Duong Thuy Anh Nguyen, Duong Tung Nguyen, and Angelia Nedić. Accelerated ab/push–pull methods for distributed optimization over time-varying directed networks. *IEEE Transactions on Control of Network Systems*, 11(3):1395–1407, 2023.
- [27] Kai Gong and Liwei Zhang. Push-pull based distributed primal-dual algorithm for coupled constrained convex optimization in multi-agent networks. *arXiv preprint arXiv:2310.15626*, 2023.
- [28] Xiangru Lian, Ce Zhang, Huan Zhang, Cho-Jui Hsieh, Wei Zhang, and Ji Liu. Can decentralized algorithms outperform centralized algorithms? a case study for decentralized parallel stochastic gradient descent. *Advances in neural information processing systems*, 30, 2017.
- [29] Kun Yuan, Bicheng Ying, Xiaochuan Zhao, and Ali H Sayed. Exact diffusion for distributed optimization and learning—part i: Algorithm development. *IEEE Transactions on Signal Processing*, 67(3):708–723, 2018.
- [30] Zhi Li, Wei Shi, and Ming Yan. A decentralized proximal-gradient method with network independent step-sizes and separated convergence rates. *IEEE Transactions on Signal Processing*, 67(17):4494–4506, 2019.
- [31] Jinming Xu, Shanying Zhu, Yeng Chai Soh, and Lihua Xie. Augmented distributed gradient methods for multi-agent optimization under uncoordinated constant stepsizes. In *IEEE Conference on Decision and Control (CDC)*, pages 2055–2060, Osaka, Japan, 2015.
- [32] P. Di Lorenzo and G. Scutari. Next: In-network nonconvex optimization. *IEEE Transactions on Signal and Information Processing over Networks*, 2(2):120–136, 2016.
- [33] G. Qu and N. Li. Harnessing smoothness to accelerate distributed optimization. *IEEE Transactions on Control of Network Systems*, 5(3):1245–1260, 2018.

- [34] Shi Pu and Angelia Nedić. Distributed stochastic gradient tracking methods. *Mathematical Programming*, 187(1):409–457, 2021.
- [35] Kun Yuan, Sulaiman A Alghunaim, Bicheng Ying, and Ali H Sayed. On the influence of bias-correction on distributed stochastic optimization. *IEEE Transactions on Signal Processing*, 68:4352–4367, 2020.
- [36] Anastasia Koloskova, Nicolas Loizou, Sadra Boreiri, Martin Jaggi, and Sebastian Stich. A unified theory of decentralized sgd with changing topology and local updates. In *International Conference on Machine Learning*, pages 5381–5393. PMLR, 2020.
- [37] Vyacheslav Kungurtsev, Mahdi Morafah, Tara Javidi, and Gesualdo Scutari. Decentralized asynchronous non-convex stochastic optimization on directed graphs. *IEEE Transactions on Control of Network Systems*, 2023.
- [38] Liyuan Liang, Xinmeng Huang, Ran Xin, and Kun Yuan. Towards better understanding the influence of directed networks on decentralized stochastic optimization. *arXiv preprint arXiv:2312.04928*, 2023.
- [39] Liyuan Liang, Xinyi Chen, Gan Luo, and Kun Yuan. Achieving linear speedup and near-optimal complexity for decentralized optimization over row-stochastic networks. *arXiv preprint arXiv:2506.04600*, 2025.
- [40] Ran Xin, Anit Kumar Sahu, Usman A Khan, and Soumya Kar. Distributed stochastic optimization with gradient tracking over strongly-connected networks. In *2019 IEEE 58th Conference on Decision and Control (CDC)*, pages 8353–8358. IEEE, 2019.
- [41] Runze You and Shi Pu. Distributed learning over arbitrary topology: Linear speed-up with polynomial transient time. *arXiv preprint arXiv:2503.16123*, 2025.
- [42] Oskar Perron. Zur theorie der matrices. *Mathematische Annalen*, 64(2):248–263, 1907.
- [43] A. Nedic, A. Olshevsky, and W. Shi. Achieving geometric convergence for distributed optimization over time-varying graphs. *SIAM Journal on Optimization*, 27(4):2597–2633, 2017.
- [44] Guannan Qu and Na Li. Harnessing smoothness to accelerate distributed optimization. *IEEE Transactions on Control of Network Systems*, 5(3):1245–1260, 2017.
- [45] Angelia Nedić and Alex Olshevsky. Stochastic gradient-push for strongly convex functions on time-varying directed graphs. *IEEE Transactions on Automatic Control*, 61(12):3936–3947, 2016.
- [46] Fakhteh Saadatniaki, Ran Xin, and Usman A Khan. Decentralized optimization over time-varying directed graphs with row and column-stochastic matrices. *IEEE Transactions on Automatic Control*, 65(11):4769–4780, 2020.

## A Rolling-Sum Lemma

**Lemma 6** (ROLLING SUM LEMMA). *For a row-stochastic weight matrix satisfying Proposition 1, the following inequality holds for any  $T \geq 0$ :*

$$\sum_{k=0}^T \left\| \sum_{i=0}^k (A^{k-i} - A_\infty) \Delta^{(i)} \right\|_F^2 \leq s_A^2 \sum_{i=0}^T \|\Delta^{(i)}\|_F^2, \quad (18)$$

where  $\Delta^{(i)} \in \mathbb{R}^{n \times d}$  are arbitrary matrices,  $s_A$  is defined as in (2). Furthermore, if Assumption 1 and 2 hold, we have

$$s_A := \max \left\{ \sum_{i=0}^{\infty} \|A^i - A_\infty\|_2, \sum_{i=0}^{\infty} \|A^i - A_\infty\|_2^2 \right\} \leq \frac{M_A^2 (1 + \frac{1}{2} \ln(\kappa_A))}{1 - \beta_A}.$$

where  $\beta_A, \kappa_A, M_A$  are defined in Proposition 2. The row-stochastic matrix  $A$  and the subscript  $A$  can be replaced by a column-stochastic matrix  $B$  without changing the lemma.

*Proof.* First, we prove that

$$\|A^i - A_\infty\|_2 \leq \sqrt{\kappa_A} \beta_A^i, \forall i \geq 0. \quad (19)$$

Notice that  $\beta_A := \|A - A_\infty\|_{\pi_A}$  and

$$\|A^i - A_\infty\|_{\pi_A} = \|(A - A_\infty)^i\|_{\pi_A} \leq \|A - A_\infty\|_{\pi_A}^i = \beta_A^i,$$

we have

$$\|(A^i - A_\infty)v\| = \|\Pi_A^{-1/2}(A^i - A_\infty)v\|_{\pi_A} \leq \sqrt{\pi_A} \beta_A^i \|v\|_{\pi_A} \leq \sqrt{\kappa_A} \beta_A^i \|v\|,$$

where  $\pi_A := \min \pi_A, \bar{\pi}_A := \max \pi_A$ . The last inequality comes from  $\|v\|_{\pi_A} \leq \bar{\pi}_A \|v\|$ . Therefore, (19) holds.

Second, we want to prove that

$$s_A \leq \frac{M_A^2 (1 + \frac{1}{2} \ln(\kappa_A))}{1 - \beta_A}. \quad (20)$$

Towards this end, we define  $M_A := \max\{1, \max_{k \geq 0} \|A^k - A_\infty\|_2\}$ . According to (19),  $M_A$  is well-defined. We also

define  $p = \max \left\{ \frac{\ln(\sqrt{\kappa_A}) - \ln(M_A)}{-\ln(\beta_A)}, 0 \right\}$ , then we can verify that  $\|A^i - A_\infty\|_2 \leq \min\{M_A, M_A \beta_A^{i-p}\}, \forall i \geq 0$ .

With this inequality, we can bound  $\sum_{i=0}^k \|A^{k+1-i} - A_\infty\|_2$  as follows:

$$\begin{aligned} \sum_{i=0}^k \|A^{k-i} - A_\infty\|_2 &= \sum_{i=0}^{\min\{\lfloor p \rfloor, k\}} \|A^i - A_\infty\|_2 + \sum_{i=\min\{\lfloor p \rfloor, k\}+1}^k \|A^i - A_\infty\|_2 \\ &\leq \sum_{i=0}^{\min\{\lfloor p \rfloor, k\}} M_A + \sum_{i=\min\{\lfloor p \rfloor, k\}+1}^k M_A \beta_A^{i-p} \\ &\leq M_A \cdot (1 + \min\{\lfloor p \rfloor, k\}) + M_A \cdot \frac{1}{1 - \beta_A} \beta_A^{\min\{\lfloor p \rfloor, k\}+1-p}. \end{aligned} \quad (21)$$

If  $p = 0$ , (21) is simplified to  $\sum_{i=0}^k \|A^{k-i} - A_\infty\|_2 \leq M_A \cdot \frac{1}{1 - \beta_A}$  and (20) is naturally satisfied. If  $p > 0$ , let  $x = \min\{\lfloor p \rfloor, k\} + 1 - p \in [0, 1]$ , (20) is simplified to

$$\sum_{i=0}^k \|A^{k-i} - A_\infty\|_2 \leq M_A(x + p + \frac{\beta_A^x}{1 - \beta_A}) \leq M_A(p + \frac{1}{1 - \beta_A}) = \frac{M_A(1 + \frac{1}{2} \ln(\kappa_A))}{1 - \beta_A}.$$

By the definition of  $p$ , we have  $p \leq \frac{\frac{1}{2} \ln(\kappa_A)}{1 - \beta_A}$ . This completes the estimation of  $\sum_{i=0}^\infty \|A^{k-i} - A_\infty\|_2$ . For the summation of the squared norm, we can use the same  $p$  and obtain the upper bound without modifying the previous steps:

$$\sum_{i=0}^k \|A^{k-i} - A_\infty\|_2^2 \leq M_A^2(p + \frac{1}{1 - \beta_A}) = \frac{M_A^2(1 + \frac{1}{2} \ln(\kappa_A))}{1 - \beta_A}.$$

This finishes the proof of (20).

Finally, to obtain (18), we use Jensen's inequality. For any positive numbers  $a_0, a_1, \dots, a_k$  satisfying  $\sum_{i=0}^k a_i = 1$ , we have

$$\begin{aligned} \left\| \sum_{i=0}^k (A^{k-i} - A_\infty) \Delta^{(i)} \right\|_F^2 &= \left\| \sum_{i=0}^k a_{k-i} \cdot a_{k-i}^{-1} (A^{k-i} - A_\infty) \Delta^{(i)} \right\|_F^2 \\ &\leq \sum_{i=0}^k a_{k-i} \|a_{k-i}^{-1} (A^{k-i} - A_\infty) \Delta^{(i)}\|_F^2 \leq \sum_{i=0}^k a_{k-i}^{-1} \|A^{k-i} - A_\infty\|_2^2 \|\Delta^{(i)}\|_F^2. \end{aligned} \quad (22)$$

By choosing  $a_{k-i} = (\sum_{i=0}^k \|A^{k-i} - A_\infty\|_2)^{-1} \|A^{k-i} - A_\infty\|_2$  in (22), we obtain that

$$\left\| \sum_{i=0}^k (A^{k-i} - A_\infty) \Delta^{(i)} \right\|_F^2 \leq \sum_{i=0}^k \|A^{k-i} - A_\infty\|_2 \cdot \sum_{i=0}^k \|A^{k-i} - A_\infty\|_2 \|\Delta^{(i)}\|_F^2. \quad (23)$$

By summing up (23) from  $k = 0$  to  $T$ , we obtain that

$$\begin{aligned} \sum_{k=0}^T \left\| \sum_{i=0}^k (A^{k-i} - A_\infty) \Delta^{(i)} \right\|_F^2 &\leq s_A \sum_{k=0}^T \sum_{i=0}^k \|A^{k-i} - A_\infty\|_2 \|\Delta^{(i)}\|_F^2 \\ &\leq s_A \sum_{i=0}^T \left( \sum_{k=i}^T \|A^{k-i} - A_\infty\|_2 \right) \|\Delta^{(i)}\|_F^2 \leq s_A^2 \sum_{i=0}^T \|\Delta^{(i)}\|_F^2, \end{aligned}$$

which finishes the proof of this lemma.  $\square$

## B Proofs of Main Theorem

### B.1 Proof of Lemma 4

For simplicity, we define  $\Delta_y^{(k)} := (I - B_\infty) \mathbf{y}^{(k)}$  and  $\overline{\nabla} f^{(k)} := \frac{1}{n} \sum_{i=1}^n \nabla f_i(x_i^{(k)})$ . According to Assumption 3, we have

$$\mathbb{E}_k[\bar{g}^{(k+i)}] = \mathbb{E}_k[\mathbb{E}_{k+i}[\bar{g}^{(k+i)}]] = \mathbb{E}_k[\overline{\nabla} f^{(k+i)}], \quad \forall i \geq 0.$$

Note that

$$\pi_A^\top \sum_{i=0}^{m-1} \mathbf{y}^{(k+i)} = c \sum_{i=0}^{m-1} \bar{g}^{(k+i)} + \pi_A^\top \sum_{i=0}^{m-1} \Delta_y^{(k+i)},$$

the descent lemma on  $\hat{x}^{(k+m)} = \hat{x}^{(k)} - \alpha \pi_A^\top \sum_{i=k}^{k+m-1} \mathbf{y}^{(i)}$  can be written as follows:

$$\begin{aligned} f(\hat{x}^{(k+m)}) - f(\hat{x}^{(k)}) &\leq -c\alpha \left\langle \sum_{i=0}^{m-1} \bar{g}^{(k+i)}, \nabla f(\hat{x}^{(k)}) \right\rangle - \alpha \left\langle \pi_A^\top \sum_{i=0}^{m-1} \Delta_y^{(k+i)}, \nabla f(\hat{x}^{(k)}) \right\rangle \\ &\quad + c^2 \alpha^2 L \left\| \sum_{i=0}^{m-1} \bar{g}^{(k+i)} \right\|^2 + \alpha^2 L \left\| \pi_A^\top \sum_{i=0}^{m-1} \Delta_y^{(k+i)} \right\|^2. \end{aligned}$$

By taking expectation conditioned on  $\mathcal{F}_k$ , we obtain that

$$\begin{aligned} \mathbb{E}_k[f(\hat{x}^{(k+m)})] - f(\hat{x}^{(k)}) &\leq -c\alpha \sum_{i=0}^{m-1} \mathbb{E}_k \left[ \left\langle \bar{\nabla} f^{(k+i)}, \nabla f(\hat{x}^{(k)}) \right\rangle \right] \\ &\quad - \alpha \mathbb{E}_k \left[ \left\langle \pi_A^\top \sum_{i=0}^{m-1} \Delta_y^{(k+i)}, \nabla f(\hat{x}^{(k)}) \right\rangle \right] + c^2 \alpha^2 L \mathbb{E}_k \left[ \left\| \sum_{i=0}^{m-1} \bar{g}^{(k+i)} \right\|^2 \right] \\ &\quad + \alpha^2 L \mathbb{E}_k \left[ \left\| \pi_A^\top \sum_{i=0}^{m-1} \Delta_y^{(k+i)} \right\|^2 \right]. \end{aligned} \tag{24}$$

The first inner product term in (24) can be bounded by:

$$\begin{aligned} - \left\langle \bar{\nabla} f^{(k+i)}, \nabla f(\hat{x}^{(k)}) \right\rangle &= -\frac{1}{2} \|\bar{\nabla} f^{(k+i)}\|^2 - \frac{1}{2} \|\nabla f(\hat{x}^{(k)})\|^2 + \frac{1}{2} \|\bar{\nabla} f^{(k+i)} - \nabla f(\hat{x}^{(k)})\|^2 \\ &\leq -\frac{1}{2} \|\bar{\nabla} f^{(k+i)}\|^2 - \frac{1}{2} \|\nabla f(\hat{x}^{(k)})\|^2 + \frac{L^2}{2} \|\mathbf{x}^{(k+i)} - \hat{\mathbf{x}}^{(k)}\|_F^2, \end{aligned}$$

where the last inequality comes from Cauchy-Schwarz inequality and  $L$ -smoothness. The first quartic term in (24) can be bounded by:

$$\mathbb{E}_k \left[ \left\| \sum_{i=0}^{m-1} \bar{g}^{(k+i)} \right\|^2 \right] \leq n^{-1} m \sigma^2 + \mathbb{E}_k \left[ \left\| \sum_{i=0}^{m-1} \bar{\nabla} f^{(k+i)} \right\|^2 \right],$$

where we use the fact that  $\bar{g}^{(k+i)}$  are conditionally unbiased estimates and

$$\mathbb{E}_k \left[ \left\langle \bar{g}^{(k+i)} - \bar{\nabla} f^{(k+i)}, \bar{g}^{(k+j)} - \bar{\nabla} f^{(k+j)} \right\rangle \right] = 0.$$

Plug these estimations into (24), we obtain that

$$\begin{aligned} &\frac{\alpha c m}{2} \mathbb{E}_k [\|\nabla f(\hat{x}^{(k)})\|^2] + \frac{\alpha c}{2} \sum_{i=0}^{m-1} \mathbb{E}_k [\|\bar{\nabla} f^{(k+i)}\|^2] \leq \mathbb{E}_k [f(\hat{x}^{(k)}) - f(\hat{x}^{(k+m)})] \\ &\quad + \frac{c \alpha L^2}{2} \sum_{i=0}^{m-1} \mathbb{E}_k [\|\mathbf{x}^{(k+i)} - \hat{\mathbf{x}}^{(k)}\|_F^2] + \frac{\alpha^2 c^2 m L}{n} \sigma^2 + c^2 \alpha^2 L \mathbb{E}_k \left[ \left\| \sum_{i=0}^{m-1} \bar{\nabla} f^{(k+i)} \right\|^2 \right] \\ &\quad - \alpha \mathbb{E} \left[ \left\langle \pi_A^\top \sum_{i=0}^{m-1} \Delta_y^{(k+i)}, \nabla f(\hat{x}^{(k)}) \right\rangle \right] + \alpha^2 L \mathbb{E}_k \left[ \left\| \pi_A^\top \sum_{i=0}^{m-1} \Delta_y^{(k+i)} \right\|^2 \right]. \end{aligned} \tag{25}$$

Next, we try to simplify the last quadratic term in (25). Notice that

$$\sum_{i=0}^{m-1} \Delta_y^{(k+i)} = \left( \sum_{j=0}^{m-1} (B^j - B_\infty) \right) \Delta_y^{(k)} + \sum_{j=1}^{m-1} (B^{m-j-1} - B_\infty) (\mathbf{g}^{(k+j)} - \mathbf{g}^{(k)}),$$

the quadratic term can be bounded as:

$$\begin{aligned} \mathbb{E}_k[\|\pi_A^\top \sum_{i=0}^{m-1} \Delta_y^{(k+i)}\|^2] &\leq \mathbb{E}_k[\|\sum_{i=0}^{m-1} \Delta_y^{(k+i)}\|_F^2] \\ &\leq 2\|\sum_{j=0}^{m-1} (B^j - B_\infty)\|_2^2 \mathbb{E}_k[\|\Delta_y^{(k)}\|_F^2] + 2\mathbb{E}_k[\|\sum_{j=1}^{m-1} (B^{m-j-1} - B_\infty)(\mathbf{g}^{(k+j)} - \mathbf{g}^{(k)})\|_F^2]. \end{aligned} \quad (26)$$

The first term here can be estimated using the fact that  $\|\sum_{j=0}^{m-1} (B^j - B_\infty)\|_2^2 \leq s_B^2$ . For the second term in (26), according to Assumption 3, we have

$$\begin{aligned} &\mathbb{E}_k[\|\sum_{j=1}^{m-1} (B^{m-j-1} - B_\infty)(\mathbf{g}^{(k+j)} - \mathbf{g}^{(k)})\|_F^2] \\ &= \sum_{j=1}^{m-1} \mathbb{E}_k[\|(B^{m-j-1} - B_\infty)(\mathbf{g}^{(k+j)} - \nabla f(\mathbf{x}^{(k+j)}))\|_F^2] \\ &\quad + \mathbb{E}_k[\| \left( \sum_{j=1}^{m-1} (B^{m-j-1} - B_\infty) \right) (\mathbf{g}^{(k)} - \nabla f(\mathbf{x}^{(k)})) \|_F^2] \\ &\quad + \mathbb{E}_k[\|\sum_{j=1}^{m-1} (B^{m-j-1} - B_\infty)(\nabla f(\mathbf{x}^{(k+j)}) - \nabla f(\mathbf{x}^{(k)}))\|_F^2] \\ &\leq n\sigma^2 \sum_{j=1}^{m-1} \|B^{m-j-1} - B_\infty\|_2^2 + n\sigma^2 \|\sum_{j=1}^{m-1} (B^{m-j-1} - B_\infty)\|_2^2 \\ &\quad + \mathbb{E}_k[\|\sum_{j=1}^{m-1} (B^{m-j-1} - B_\infty)(\nabla f(\mathbf{x}^{(k+j)}) - \nabla f(\mathbf{x}^{(k)}))\|_F^2] \\ &\leq 2ns_B^2\sigma^2 + \mathbb{E}_k[\|\sum_{j=1}^{m-1} (B^{m-j-1} - B_\infty)(\nabla f(\mathbf{x}^{(k+j)}) - \nabla f(\mathbf{x}^{(k)}))\|_F^2] \end{aligned} \quad (27)$$

The inner product can produce a similar term:

$$\mathbb{E}_k[\pi_A^\top \sum_{i=0}^{m-1} \Delta_y^{(k+i)}] = \mathbb{E}_k[H_{m,k}].$$

Using the fact that  $\hat{x}^{(k)}$  is known under filtration  $\mathcal{F}_k$ , we have

$$\begin{aligned}
& -\alpha \mathbb{E}_k \left[ \left\langle \pi_A^\top \sum_{i=0}^{m-1} \Delta_y^{(k+i)}, \nabla f(\hat{x}^{(k)}) \right\rangle \right] = -\alpha \left\langle \mathbb{E}_k[H_{m,k}], \nabla f(\hat{x}^{(k)}) \right\rangle \\
& = -\alpha \left\langle \mathbb{E}_k \left[ \pi_A^\top \sum_{j=1}^{m-1} (B^{m-j-1} - B_\infty) (\nabla f(\mathbf{x}^{(k+j)}) - \nabla f(\mathbf{x}^{(k)})) \right], \nabla f(\hat{x}^{(k)}) \right\rangle \\
& \quad + \alpha \left\langle \pi_A^\top \left( \sum_{i=0}^{m-1} (B^{m-i-1} - B_\infty) \right) \Delta_y^{(k)}, \nabla f(\hat{x}^{(k)}) \right\rangle \\
& \stackrel{\text{Cauchy}}{\leq} \frac{2\alpha}{cm} \mathbb{E}_k \left[ \left\| \pi_A^\top \sum_{j=1}^{m-1} (B^{m-j-1} - B_\infty) (\nabla f(\mathbf{x}^{(k+j)}) - \nabla f(\mathbf{x}^{(k)})) \right\|^2 \right] + \frac{\alpha cm}{8} \|\nabla f(\hat{x}^{(k)})\|^2 \\
& \quad + \frac{2\alpha}{cm} \left\| \pi_A^\top \left( \sum_{i=0}^{m-1} (B^{m-i-1} - B_\infty) \right) \Delta_y^{(k)} \right\|_F^2 + \frac{\alpha cm}{8} \|\nabla f(\hat{x}^{(k)})\|^2 \\
& \leq \frac{2\alpha}{cm} \mathbb{E}_k \left[ \left\| \sum_{j=1}^{m-1} (B^{m-j-1} - B_\infty) (\nabla f(\mathbf{x}^{(k+j)}) - \nabla f(\mathbf{x}^{(k)})) \right\|_F^2 \right] + \frac{\alpha cm}{4} \|\nabla f(\hat{x}^{(k)})\|^2 \\
& \quad + \frac{2\alpha s_B^2}{cm} \|\Delta_y^{(k)}\|_F^2,
\end{aligned} \tag{28}$$

where the last inequality uses  $\|\pi_A\| \leq 1$  and  $\left\| \sum_{j=1}^{m-1} (B^{m-j-1} - B_\infty) \right\|_2 \leq s_B$ . Plug (26) and (28) into (25), we obtain that

$$\begin{aligned}
& \frac{\alpha cm}{4} \mathbb{E}_k [\|\nabla f(\hat{x}^{(k)})\|^2] + \frac{\alpha c}{2} \sum_{i=0}^{m-1} \mathbb{E}_k [\|\overline{\nabla f}^{(k+i)}\|^2] - c^2 \alpha^2 L \mathbb{E}_k \left[ \left\| \sum_{i=0}^{m-1} \overline{\nabla f}^{(k+i)} \right\|^2 \right] \\
& \leq \mathbb{E}_k [f(\hat{x}^{(k)}) - f(\hat{x}^{(k+m)})] + \frac{c\alpha L^2}{2} \sum_{i=0}^{m-1} \mathbb{E} [\|\mathbf{x}^{(k+i)} - \hat{\mathbf{x}}^{(k)}\|_F^2] \\
& \quad + \frac{2\alpha^2 c^2 mL}{n} \sigma^2 + 2\alpha^2 L n s_B^2 \sigma^2 + (2\alpha^2 L s_B^2 + \frac{2\alpha s_B^2}{cm}) \mathbb{E} [\|\Delta_y^{(k)}\|_F^2] \\
& \quad + (2\alpha^2 L + \frac{2\alpha}{cm}) \mathbb{E} \left[ \left\| \sum_{j=1}^{m-1} (B^{m-j-1} - B_\infty) (\nabla f(\mathbf{x}^{(k+j)}) - \nabla f(\mathbf{x}^{(k)})) \right\|_F^2 \right]
\end{aligned} \tag{29}$$

For  $c^2 \alpha^2 L \mathbb{E} [\left\| \sum_{i=0}^{m-1} \overline{\nabla f}^{(k+i)} \right\|^2]$ , we have the following estimate:

$$\mathbb{E} \left[ \left\| \sum_{i=0}^{m-1} \overline{\nabla f}^{(k+i)} \right\|^2 \right] \leq m \sum_{i=0}^{m-1} \mathbb{E} [\|\overline{\nabla f}^{(k+i)}\|^2]. \tag{30}$$

Take (30) into (29), and suppose  $\alpha \leq \frac{1}{4cmL}$ , we obtain that

$$\begin{aligned}
& \frac{\alpha cm}{4} \mathbb{E}[\|\nabla f(\hat{x}^{(k)})\|^2] + \frac{\alpha c}{4} \sum_{i=0}^{m-1} \mathbb{E}[\|\overline{\nabla f}^{(k+i)}\|^2] \\
& \leq \mathbb{E}[f(\hat{x}^{(k)}) - f(\hat{x}^{(k+m)})] + \frac{c\alpha L^2}{2} \sum_{i=0}^{m-1} \mathbb{E}[\|\mathbf{x}^{(k+i)} - \hat{\mathbf{x}}^{(k)}\|_F^2] \\
& + \frac{2\alpha^2 c^2 mL}{n} \sigma^2 + 2\alpha^2 L n s_B^2 \sigma^2 + \frac{3\alpha s_B^2}{cm} \mathbb{E}[\|\Delta_y^{(k)}\|_F^2] \\
& + \frac{3\alpha}{cm} \mathbb{E}[\|\sum_{j=1}^{m-1} (B^{m-j-1} - B_\infty)(\nabla f(\mathbf{x}^{(k+j)}) - \nabla f(\mathbf{x}^{(k)}))\|_F^2]
\end{aligned} \tag{31}$$

We can further apply Cauchy's inequality on the last term in (31), i.e.

$$\begin{aligned}
& \|\sum_{j=1}^{m-1} (B^{m-j-1} - B_\infty)(\nabla f(\mathbf{x}^{(k+j)}) - \nabla f(\mathbf{x}^{(k)}))\|_F^2 \\
& \leq \sum_{j=1}^{m-1} \|B^{m-j-1} - B_\infty\|_2^2 \sum_{j=1}^{m-1} \|\nabla f(\mathbf{x}^{(k+j)}) - \nabla f(\mathbf{x}^{(k)})\|_F^2 \\
& \leq s_B \sum_{j=1}^{m-1} \|\nabla f(\mathbf{x}^{(k+j)}) - \nabla f(\mathbf{x}^{(k)})\|_F^2 \leq s_B L^2 \sum_{j=1}^{m-1} \|\mathbf{x}^{(k+j)} - \mathbf{x}^{(k)}\|_F^2.
\end{aligned}$$

Finally, when  $m \geq 6c^{-2}s_B$ , we have  $\frac{3\alpha s_B L^2}{cm} \leq \frac{c\alpha L^2}{2}$ , and (31) can be further simplified to

$$\begin{aligned}
& \frac{\alpha cm}{4} \mathbb{E}[\|\nabla f(\hat{x}^{(k)})\|^2] + \frac{\alpha c}{4} \sum_{i=0}^{m-1} \mathbb{E}[\|\overline{\nabla f}^{(k+i)}\|^2] \\
& \leq \mathbb{E}[f(\hat{x}^{(k)}) - f(\hat{x}^{(k+m)})] + \frac{c\alpha L^2}{2} \sum_{i=0}^{m-1} \mathbb{E}[\|\mathbf{x}^{(k+i)} - \hat{\mathbf{x}}^{(k)}\|_F^2] \\
& + \frac{2\alpha^2 c^2 mL}{n} \sigma^2 + 2\alpha^2 L n s_B^2 \sigma^2 + \frac{3\alpha s_B^2}{cm} \mathbb{E}[\|\Delta_y^{(k)}\|_F^2] \\
& + \frac{c\alpha L^2}{2} \sum_{j=1}^k \mathbb{E}_k[\|\mathbf{x}^{(k+j)} - \mathbf{x}^{(k)}\|_F^2],
\end{aligned}$$

which finishes the proof.

## B.2 Proof of Lemma 5

In this section, we consider how to measure the difference of  $\mathbf{x}$ . To be more specific, we mainly consider the relationships between the following 4 terms:

$$\Delta_1^{(k)}, \Delta_2^{(k)}, \mathbb{E}_k[\|\Delta_x^{(k)}\|_F^2], \Delta_y^{(k)}, \quad k \in [m^*].$$

Lemma 7 will give upper bounds of  $\Delta_1^{(k)}, \Delta_2^{(k)}$  using other terms, while Lemma



**Lemma 7.** Suppose Proposition 2 and Assumption 3, 4 hold. When  $\alpha \leq \frac{1}{6s_B L}$ ,  $m \geq \max\{c^{-2}n^2(N_7 + N_8^2), s_A^2, n^{-1}s_A, c^{-2}n^2s_A^2\}$ , the following inequalities hold for any positive integers  $k$  and  $m$ .

$$\Delta_1^{(k)} \leq 40mn\|\Delta_x^{(k)}\|_F^2 + 40\alpha^2ms_B\|\Delta_y^{(k)}\|_F^2 + 20c^2\alpha^2m^2n^{-1}\sigma^2 \quad (32)$$

$$+ 20c^2\alpha^2m^2 \sum_{j=0}^{m-1} \mathbb{E}_k[\|\overline{\nabla f}^{(k+j)}\|^2],$$

$$\Delta_2^{(k)} \leq 40mn\|\Delta_x^{(k)}\|_F^2 + 40\alpha^2ms_B\|\Delta_y^{(k)}\|_F^2 + 20c^2\alpha^2m^2n^{-1}\sigma^2 \quad (33)$$

$$+ 20c^2\alpha^2m^2 \sum_{j=0}^{m-1} \mathbb{E}_k[\|\overline{\nabla f}^{(k+j)}\|^2],$$

*Proof.* Define  $\delta_B^{(0)} = I - B_\infty$ ,  $\delta_B^{(j)} = B^j - B^{j-1}$ , when  $j \geq 1$ . We have

$$\begin{aligned} \mathbf{x}^{(k+i)} - \hat{\mathbf{x}}^{(k)} - (A^i - A_\infty)\Delta_x^{(k)} &= -\alpha \sum_{j=0}^{i-1} A^{i-j-1} \Delta_y^{(k+j)} - \alpha \sum_{j=0}^{i-1} A^{i-j-1} B_\infty \mathbf{y}^{(k+j)} \\ &= -\alpha \sum_{j=1}^{i-1} A^{i-j-1} (B^j - B_\infty) \Delta_y^{(k)} - \alpha \sum_{l=1}^{i-1} \sum_{j=0}^{i-l-1} A^{i-j-l-1} \delta_B^{(j)} (\mathbf{g}^{(k+l)} - \mathbf{g}^{(k)}) \\ &\quad - \alpha \sum_{j=0}^{i-1} (A^{i-j-1} - A_\infty) n \pi_B \bar{g}^{(k+j)} - \alpha c \sum_{j=0}^{i-1} \bar{g}^{(k+j)}. \end{aligned}$$

Therefore, we can apply Cauchy's inequality and sum it up from  $i = 1$  to  $m - 1$ :

$$\begin{aligned} &\sum_{i=1}^{m-1} \mathbb{E}_k[\|\mathbf{x}^{(k+i)} - \hat{\mathbf{x}}^{(k)}\|_F^2] \\ &\leq 5 \sum_{i=1}^{m-1} \|A^i - A_\infty\|_2^2 \|\Delta_x^{(k)}\|_F^2 + 5\alpha^2 \sum_{i=1}^{m-1} \left\| \sum_{j=1}^{i-1} A^{i-j-1} (B^j - B_\infty) \right\|_2^2 \|\Delta_y^{(k)}\|_F^2 \\ &\quad + 5\alpha^2 \sum_{i=1}^{m-1} \left( \sum_{l=1}^{i-1} \left\| \sum_{j=0}^{i-l-1} A^{i-j-l-1} \delta_B^{(j)} \right\|_2^2 + \left\| \sum_{l=1}^{i-1} \sum_{j=0}^{i-l-1} A^{i-j-l-1} \delta_B^{(j)} \right\|_2^2 \right) n \sigma^2 \\ &\quad + 5\alpha^2 \sum_{i=1}^{m-1} \mathbb{E}_k[\left\| \sum_{j=l}^{i-1} A^{i-j-1} \delta_B^{(j-l)} (\nabla f(\mathbf{x}^{(k+l)}) - \nabla f(\mathbf{x}^{(k)})) \right\|_F^2] \\ &\quad + 5\alpha^2 n^2 s_A^2 \sum_{i=1}^{m-1} \|\overline{\nabla f}^{(k+i)}\|^2 + 5\alpha^2 n \sum_{i=1}^{m-1} \sum_{j=0}^{i-1} \|A^{i-j-1} - A_\infty\|_2^2 \\ &\quad + 5c^2\alpha^2m^2 \sum_{j=0}^{m-1} \|\overline{\nabla f}^{(k+j)}\|^2 + 5c^2\alpha^2m^2n^{-1}\sigma^2 \\ &\leq 5s_A\|\Delta_x^{(k)}\|_F^2 + 10\alpha^2(s_A^2s_B + ms_B)\|\Delta_y^{(k)}\|_F^2 + 5\alpha^2m(N_7 + N_8^2 + c^2mn^{-2})n\sigma^2 \\ &\quad + 5\alpha^2N_8^2L^2\Delta_2^{(k)} + 5\alpha^2(n^2s_A^2 + c^2m^2)\|\overline{\nabla f}^{(k+j)}\|^2. \end{aligned}$$

where in the first inequality, the  $\sigma^2$  terms are separated using Lemma 3, and the second inequality comes

from rolling sum.

$$N_7 := \sum_{t=0}^{\infty} \left\| \sum_{j=0}^t A^{t-j} \delta_B^{(j)} \right\|_2^2 \leq 8s_A^2 s_B + 2n \|\pi_A\|^2 s_B$$

$$N_8 := \sum_{t=0}^{\infty} \left\| \sum_{j=0}^t A^{t-j} \delta_B^{(j)} \right\|_2 \leq 2s_A s_B + \sqrt{n} \|\pi_A\| s_B$$

For the decomposition of  $\mathbf{x}^{(k+i)} - \mathbf{x}^{(k)}$ , the only difference is that we replace  $(A^i - A_\infty)\Delta_x^{(k)}$  with  $(A^i - I)\Delta_x^{(k)}$ .

This gives

$$\begin{aligned} \Delta_2^{(k)} &\leq 5 \sum_{i=1}^m \|A^i - I\|_2^2 \|\Delta_x^{(k)}\|_F^2 + 10\alpha^2 (s_A^2 + m) s_B \|\Delta_y^{(k)}\|_F^2 + 5\alpha^2 m (N_7 + N_8^2 + c^2 m n^{-2}) n \sigma^2 \\ &\quad + 5\alpha^2 N_8^2 L^2 \Delta_2^{(k)} + 5\alpha^2 (n^2 s_A^2 + c^2 m^2) \|\nabla f^{(k+j)}\|^2. \end{aligned}$$

Easy to prove that  $\sum_{i=1}^m \|A^i - I\|_2^2 \leq 2s_A + 2mn$ . When  $\alpha \leq \frac{1}{5N_8 L}$ , we have

$$\begin{aligned} \Delta_2^{(k)} &\leq 20(s_A + mn) \|\Delta_x^{(k)}\|_F^2 + 20\alpha^2 (s_A^2 + m) s_B \|\Delta_y^{(k)}\|_F^2 \\ &\quad + 10\alpha^2 m (N_7 + N_8^2 + c^2 m n^{-2}) n \sigma^2 + 10\alpha^2 (n^2 s_A^2 + c^2 m^2) \|\nabla f^{(k+j)}\|^2. \end{aligned} \tag{34}$$

Plug (34) into the estimate for  $\Delta_1^{(k)}$ , it is not difficult to verify that  $\Delta_1^{(k)}$  could use the same upper bound as (34).

□

Next, we provide some inequalities for the consensus error  $\Delta_x^{(k)}$  and  $\Delta_y^{(k)}$ ,  $k \in [m^*]$ .

For  $k \in [m^*]$ , we have

$$\Delta_y^{(k+m)} = (B^m - B_\infty) \Delta_y^{(k)} + \sum_{i=0}^{m-1} (B^{m-1-i} - B_\infty) (\mathbf{g}^{(k+i+1)} - \mathbf{g}^{(k+i)}) \tag{35}$$

Define

$$\Delta_3^{(k)} = \sum_{i=0}^{m-1} (B^{m-1-i} - B_\infty) (\mathbf{g}^{(k+i+1)} - \mathbf{g}^{(k+i)}).$$

Note that it can be rewritten as

$$\begin{aligned} \Delta_3^{(k)} &= (I - B_\infty) \mathbf{g}^{(k+m)} + (B - I) \mathbf{g}^{(k+m-1)} + (B^2 - B) \mathbf{g}^{(k+m-2)} \\ &\quad + \dots + (B^{m-1} - B^{m-2}) \mathbf{g}^{(k+1)} - (B^{m-1} - B_\infty) \mathbf{g}^{(k)}, \end{aligned}$$

according to Lemma 3, we have

$$\mathbb{E}_k [\|\Delta_3^{(k)}\|_F^2] \leq n\sigma^2 q_B + h_{m,k}$$

where

$$\begin{aligned} h_{m,k} &:= \sum_{j=1}^m \delta_B^{(m-j)} \nabla f(\mathbf{x}^{(k+j)}) - (B^{m-1} - B_\infty) \nabla f(\mathbf{x}^{(k)}), \\ q_B &= \sum_{j=1}^m \|\delta_B^{(m-j)}\|_2^2 + \|B^{m-1} - B_\infty\|_2^2 \leq 2s_B. \end{aligned}$$

For  $h_{m,k}$ , we can rearrange it as

$$h_{m,k} = \sum_{j=1}^m \delta_B^{(m-j)} (\nabla f(\mathbf{x}^{(k+j)}) - \nabla f(\mathbf{x}^{(k)})).$$

By applying the rolling sum lemma, we have

$$\begin{aligned} \mathbb{E}_k[\|h_{m,k}\|_F^2] &\leq \sum_{t=0}^m \|\delta_B^{(t)}\|_2^2 \sum_{j=1}^m \mathbb{E}_k[\|\nabla f(\mathbf{x}^{(k+j)}) - \nabla f(\mathbf{x}^{(k)})\|_F^2] \\ &\leq 2s_B L^2 \sum_{j=1}^m \mathbb{E}_k[\|\mathbf{x}^{(k+j)} - \mathbf{x}^{(k)}\|_F^2] = 2s_B L^2 \Delta_2^{(k)}. \end{aligned}$$

Combining the estimates above, we reach that

$$\mathbb{E}_k[\|\Delta_3^{(k)}\|_F^2] \leq 2ns_B \sigma^2 + 2s_B L^2 \Delta_2^{(k)}.$$

To proceed on, we iterate (35) and obtain that

$$\Delta_y^{(k+m)} = (B^{m+k} - B_\infty) \mathbf{g}^{(0)} + \sum_{j=0}^{k/m} (B^{k-jm} - B_\infty) \Delta_3^{(jm)}.$$

Using the rolling sum lemma, we have

$$\begin{aligned} \sum_{k \in [m^*]} \mathbb{E}[\|\Delta_y^{(k+m)}\|_F^2] &\leq 2 \sum_{k \in [m^*]} \mathbb{E}[\|(B^k - B_\infty) \mathbf{g}^{(0)}\|_F^2] + 2s_{B^m}^2 \sum_{k \in [m^*]} \mathbb{E}[\mathbb{E}_k[\|\Delta_3^{(k)}\|_F^2]] \\ &\leq s_{B^m} (n\sigma^2 + 2nL\Delta) + 4ns_B s_{B^m}^2 K\sigma^2 + 4s_B s_{B^m}^2 L^2 \sum_{k \in [m^*]} \mathbb{E}[\Delta_2^{(k)}]. \end{aligned}$$

Note that

$$\mathbb{E}[\|\Delta_y^{(0)}\|_F^2] = \mathbb{E}[\|(I - B_\infty) \mathbf{g}^{(0)}\|_F^2] \leq 2(n\sigma^2 + 2nL\Delta),$$

we combine coefficients and reach that

$$\sum_{k \in [m^*]} \|\Delta_y^{(k)}\|_F^2 \leq 7s_B s_{B^m}^2 K n \sigma^2 + 6s_{B^m} n L \Delta + 4s_B s_{B^m}^2 L^2 \sum_{k \in [m^*]} \Delta_2^{(k)}.$$

Plug in (33), we have

$$\begin{aligned} (1 - 160\alpha^2 m L^2 s_B^2 s_{B^m}^2) \sum_{k \in [m^*]} \mathbb{E}[\|\Delta_y^{(k)}\|_F^2] &\leq (7s_B s_{B^m}^2 + 80c^2 m^2 n^{-1} \alpha^2 L^2 s_B s_{B^m}^2) K n \sigma^2 \\ &\quad + 6s_{B^m} n L \Delta + 160s_B s_{B^m}^2 L^2 m n \sum_{k \in [m^*]} \mathbb{E}[\|\Delta_x^{(k)}\|_F^2] + 80c^2 m^2 s_B s_{B^m}^2 \alpha^2 L^2 \sum_{t=0}^{T-1} \mathbb{E}[\|\nabla \bar{f}^{(t)}\|^2] \end{aligned}$$

When  $\alpha \leq \frac{1}{10cm\sqrt{s_B s_{B^m}^2} L}$  and  $m \geq 10c^{-2} s_B s_{B^m}$ , we have  $1 - 160\alpha^2 m L^2 s_B^2 s_{B^m}^2 \geq 0.5$ . and the coefficient of  $K n \sigma^2$  becomes smaller than  $8s_B s_{B^m}^2$ . Thus,

$$\begin{aligned} \sum_{k \in [m^*]} \mathbb{E}[\|\Delta_y^{(k)}\|_F^2] &\leq 16s_B s_{B^m}^2 K n \sigma^2 + 12s_{B^m} n L \Delta \\ &\quad + 320s_B s_{B^m}^2 L^2 m n \sum_{k \in [m^*]} \mathbb{E}[\|\Delta_x^{(k)}\|_F^2] + 160c^2 m^2 s_B s_{B^m}^2 \alpha^2 L^2 \sum_{t=0}^{T-1} \mathbb{E}[\|\nabla \bar{f}^{(t)}\|^2]. \end{aligned} \tag{36}$$

By taking this back to (33), we have

$$\begin{aligned}
\sum_{k \in [m^*]} \mathbb{E}[\Delta_2^{(k)}] &\leq 40mn(1 + 320\alpha^2 L^2 m s_B^2 s_{B^m}^2) \sum_{k \in [m^*]} \mathbb{E}[\|\Delta_x^{(k)}\|_F^2] \\
&\quad + 480\alpha^2 m s_{B^m} n L \Delta + (640m s_B^2 s_{B^m}^2 + 20c^2 m^2 n^{-2}) \alpha^2 K n \sigma^2 \\
&\quad + 20c^2 \alpha^2 m^2 (1 + 160\alpha^2 L^2 m s_B^2 s_{B^m}^2) \sum_{t=0}^{T-1} \mathbb{E}[\|\nabla \bar{f}^{(t)}\|^2]. \\
&\leq 50mn \sum_{k \in [m^*]} \mathbb{E}[\|\Delta_x^{(k)}\|_F^2] + 480\alpha^2 m s_{B^m} n L \Delta \\
&\quad + 21c^2 m^2 n^{-1} \alpha^2 K \sigma^2 + 21c^2 \alpha^2 m^2 \mathbb{E}[\|\nabla \bar{f}^{(t)}\|^2].
\end{aligned} \tag{37}$$

where the second inequality uses  $\alpha \leq \frac{1}{10cmL}$  and  $m \geq 4c^{-2} s_B^2 s_{B^m}^2 n^2$ .

For  $k \in [m^*]$ , we have

$$\Delta_x^{(k+m)} = (A^m - A_\infty) \Delta_x^{(k)} - \alpha \sum_{i=0}^{m-1} (A^{m-i} - A_\infty) \mathbf{y}^{(k+i)}. \tag{38}$$

Define

$$\Delta_4^{(k)} := \sum_{i=0}^{m-1} (A^{m-i} - A_\infty) \mathbf{y}^{(k+i)},$$

then we can iterate (38) and obtain that

$$\Delta_x^{(k+m)} = -\alpha \sum_{j=0}^{k/m} (A^{k-jm} - A_\infty) \Delta_4^{(k)}.$$

To further analyze  $\Delta_4^{(k)}$ , we expand it as

$$\begin{aligned}
\Delta_4^{(k)} &= \sum_{i=0}^{m-1} (A^{m-i} - A_\infty) \Delta_y^{(k+i)} + n \sum_{i=0}^{m-1} (A^{m-i} - A_\infty) \pi_B \bar{g}^{(k+i)} \\
&= \sum_{i=0}^{m-1} (A^{m-i} - A_\infty) (B^i - B_\infty) \Delta_y^{(k)} + n \sum_{i=0}^{m-1} (A^{m-i} - A_\infty) \pi_B \bar{g}^{(k+i)} \\
&\quad + \sum_{j=i}^{m-1} (A^{m-i} - A_\infty) \delta_B^{(j-i)} (\mathbf{g}^{(k+j)} - \mathbf{g}^{(k)}).
\end{aligned}$$

Note that

$$\begin{aligned}
\left\| \sum_{i=0}^{m-1} (A^{m-i} - A_\infty) (B^i - B_\infty) \right\|_2^2 &\leq s_A s_B, \quad \sum_{i=0}^{m-1} \|(A^{m-i} - A_\infty) \delta_B^{(j-i)}\|_2 \leq 2s_A s_B, \\
\sum_{i=0}^{m-1} \|(A^{m-i} - A_\infty) \delta_B^{(j-i)}\|_2^2 &\leq 2s_A s_B, \quad \left\| \sum_{i=0}^{m-1} (A^{m-i} - A_\infty) \delta_B^{(j-i)} \right\|_2^2 \leq 2s_A s_B.
\end{aligned}$$

Therefore, according to Lemma 3, we can separate noiseless and noisy terms in  $\sum_{i=0}^{m-1} \pi_B \bar{g}^{(k+i)}$  and  $\sum_{j=i}^{m-1} (A^{m-i} -$

$A_\infty)(B^{j-i} - B^{j-i+1})(\mathbf{g}^{(k+j)} - \mathbf{g}^{(k)})$ , then apply Jensen's inequality. This gives

$$\begin{aligned}
\mathbb{E}_k[\|\Delta_4^{(k)}\|_F^2] &\leq 3s_A s_B \|\Delta_y^{(k)}\|_F^2 + 3n^2 s_A \sum_{i=0}^{m-1} \mathbb{E}_k[\|\overline{\nabla f}^{(k+i)}\|_F^2] + 3n s_A \sigma^2 \\
&\quad + 6s_A s_B \sum_{j=i}^{m-1} \mathbb{E}_k[\|\nabla f(\mathbf{x}^{(k+j)}) - \nabla f(\mathbf{x}^{(k)})\|_F^2] + 12s_A s_B n \sigma^2 \\
&\leq 3s_A s_B \|\Delta_y^{(k)}\|_F^2 + 3n^2 s_A \sum_{i=0}^{m-1} \mathbb{E}_k[\|\overline{\nabla f}^{(k+i)}\|_F^2] \\
&\quad + 6s_A s_B L^2 \Delta_2^{(k)} + 15s_A s_B n \sigma^2.
\end{aligned}$$

Using the rolling sum lemma, we have

$$\begin{aligned}
\sum_{k \in [m^*]} \mathbb{E}[\|\Delta_x^{(k+m)}\|_F^2] &\leq \alpha^2 s_{A^m}^2 \sum_{k \in [m^*]} \mathbb{E}[\mathbb{E}_k[\|\Delta_4^{(k)}\|_F^2]] \\
&\leq 15\alpha^2 n s_A s_B s_{A^m}^2 K \sigma^2 + 3\alpha^2 n^2 s_A s_{A^m}^2 \sum_{t=0}^{T-1} \mathbb{E}[\|\overline{\nabla f}^{(t)}\|_F^2] \\
&\quad + 6\alpha^2 L^2 s_A s_B s_{A^m}^2 \sum_{k \in [m^*]} \mathbb{E}[\Delta_2^{(k)}] + 3\alpha^2 s_A s_B s_{A^m}^2 \sum_{k \in [m^*]} \mathbb{E}\|\Delta_y^{(k)}\|_F^2
\end{aligned}$$

Note that we start from consensual  $x$ , so  $\Delta_x^{(0)} = 0$ . Plug in (37) and (36) we have

$$\begin{aligned}
&(1 - 480\alpha^2 m L^2 s_A s_B s_{A^m}^2 n - 960\alpha^2 L^2 m s_A s_B^2 s_{A^m}^2 s_{B^m}^2 n) \sum_{k \in [m^*]} \mathbb{E}[\|\Delta_x^{(k)}\|_F^2] \\
&\leq (15 + 126c^2 \alpha^2 L^2 m^2 n^{-2} + 48s_B s_{B^m}^2) \alpha^2 s_A s_B s_{A^m}^2 n K \sigma^2 \\
&\quad + (3 + (126 + 480s_B s_{B^m}^2) c^2 \alpha^2 L^2 m^2) \alpha^2 n^2 s_A s_{A^m}^2 \sum_{t=0}^{T-1} \mathbb{E}[\|\overline{\nabla f}^{(t)}\|_F^2] \\
&\quad + (36 + 2880\alpha^2 L^2) s_A s_B s_{A^m}^2 s_{B^m}^2 \alpha^2 n L \Delta
\end{aligned}$$

Using  $\alpha \leq \min\{\frac{1}{10\sqrt{s_B s_{B^m}^2} c m L}, \frac{1}{6L}\}$  and  $m \geq 20c^{-2} n s_A s_B s_{A^m}^2$ , the coefficients can be simplified to

$$\begin{aligned}
\sum_{k \in [m^*]} \mathbb{E}[\|\Delta_x^{(k)}\|_F^2] &\leq 64\alpha^2 s_A s_B^2 s_{B^m}^2 s_{A^m}^2 n K \sigma^2 \\
&\quad + 7\alpha^2 n^2 s_A s_{A^m}^2 \sum_{t=0}^{T-1} \mathbb{E}[\|\overline{\nabla f}^{(t)}\|_F^2] + 416\alpha^2 s_A s_B s_{A^m}^2 s_{B^m}^2 n L \Delta
\end{aligned} \tag{39}$$

Taking (39) back to (36), we obtain that

$$\begin{aligned}
\sum_{k \in [m^*]} \mathbb{E}[\|\Delta_y^{(k)}\|_F^2] &\leq (1 + 1280\alpha^2 L^2 m n^2 s_A s_B^2 s_{B^m}^2 s_{A^m}^2) 16s_B s_{B^m}^2 K n \sigma^2 \\
&\quad + (12 + 133120\alpha^2 L^2 s_A s_B^2 s_{B^m}^2 s_{A^m}^2) s_{B^m}^2 n L \Delta \\
&\quad + 160(c^2 m^2 s_B s_{B^m}^2 + 140\alpha^2 L^2 n^2 s_A s_{A^m}^2 s_B s_{B^m}^2) \alpha^2 L^2 \sum_{t=0}^{T-1} \mathbb{E}[\|\overline{\nabla f}^{(t)}\|_F^2].
\end{aligned}$$

When  $\alpha \leq \frac{1}{10cm\sqrt{s_B s_{B^m}^2} L}$  and  $m \geq 10c^{-2}n^2 s_A s_{A^m}^2 s_B$ , we have

$$\begin{aligned} \sum_{k \in [m^*]} \mathbb{E}[\|\Delta_y^{(k)}\|_F^2] &\leq 32s_B s_{B^m}^2 K n \sigma^2 + 26s_{B^m} n L \Delta \\ &\quad + 170c^2 m^2 \alpha^2 L^2 s_B s_{B^m}^2 \sum_{t=0}^{T-1} \mathbb{E}[\|\bar{\nabla} f^{(t)}\|_F^2]. \end{aligned} \quad (40)$$

Plug (39) into (37), we obtain that

$$\begin{aligned} \sum_{k \in [m^*]} \mathbb{E}[\Delta_2^{(k)}] &\leq (21c^2 m^2 n^{-2} + 3200mn s_A s_B^2 s_{A^m}^2 s_{B^m}^2) \alpha^2 n K \sigma^2 \\ &\quad + 21280 s_A s_B s_{A^m}^2 s_{B^m}^2 \alpha^2 m n^2 L \Delta + (21c^2 m + 350n^3 s_A s_{A^m}^2) \alpha^2 m \sum_{t=0}^{T-1} \mathbb{E}[\|\bar{\nabla} f^{(t)}\|_F^2]. \\ &\leq 181c^2 m^2 n^{-1} \alpha^2 K \sigma^2 + 21280 s_A s_B s_{A^m}^2 s_{B^m}^2 \alpha^2 m n^2 L \Delta + 38\alpha^2 c^2 m^2 \sum_{t=0}^{T-1} \mathbb{E}[\|\bar{\nabla} f^{(t)}\|_F^2], \end{aligned} \quad (41)$$

where the second inequality uses  $m \geq 20c^{-2}n^3 s_A s_{A^m}^2 s_B^2 s_{B^m}^2$ . Now we are ready to estimate the summation of error terms and prove Lemma 5. Remember that  $\Delta_1^{(k)}$  and  $\Delta_2^{(k)}$  share the same upper bound, we utilize (41), (40) and obtain that

$$\begin{aligned} &\frac{c\alpha L^2}{2} \sum_{k \in [m^*]} \mathbb{E}[\Delta_1^{(k)} + \Delta_2^{(k)}] + \frac{3\alpha s_B^2}{cm} \sum_{k \in [m^*]} \mathbb{E}[\|\Delta_y^{(k)}\|_F^2] \\ &\leq \frac{\alpha cm}{4} C_{\sigma,1} K \sigma^2 + \frac{c\alpha}{4} C_{f,1} \sum_{t=0}^{T-1} \mathbb{E}[\|\bar{\nabla} f^{(t)}\|_F^2] + C_{\Delta,1} \frac{c\alpha L \Delta}{4m}, \end{aligned}$$

where

$$\begin{aligned} C_{\sigma,1} &= 724c^2 m n^{-1} \alpha^2 L^2 + \frac{384s_B^3 s_{B^m}^2}{m^2 c^2} \\ C_{f,1} &= 152c^2 \alpha^2 L^2 m^2 + 2040m \alpha^2 L^2 s_B^3 s_{B^m}^2 \\ C_{\Delta,1} &= 85120 s_A s_B s_{A^m}^2 s_{B^m}^2 \alpha^2 L^2 m^2 n^2 + \frac{312s_B^2 s_{B^m} n}{c^2}. \end{aligned}$$

When  $\alpha \leq \frac{1}{10cm\sqrt{s_B s_{B^m}^2} L}$  and  $m \geq c^{-2}30s_B^{1.5}$ , we have

$$C_{\sigma,1} \leq \frac{73c\alpha L}{n} + \frac{384s_B^3 s_{B^m}^2}{m^2 c^2}, \quad C_{f,1} \leq 1, \quad C_{\Delta,1} \leq \frac{10s_A s_{A^m}^2 n^2 + 312s_B^2 s_{B^m} n}{c^2}.$$

This finishes the proof.

### B.3 Proof of Theorem 1

Sum up Lemma 4 for  $k \in [m^*]$ , then plug in Lemma 5, we obtain that

$$\begin{aligned} &\frac{\alpha cm}{4} \sum_{k \in [m^*]} \mathbb{E}[\|\nabla f(\hat{x}^{(k)})\|^2] + \frac{\alpha c}{4} (1 - C_{f,1}) \sum_{t=0}^{T-1} \mathbb{E}[\|\bar{\nabla} f^{(t)}\|^2] \\ &\leq f(x^{(0)}) - f(\hat{x}^T) + \frac{\alpha cm}{4} \left( \frac{8\alpha c L}{n} + \frac{8\alpha L n s_B^2}{cm} + C_{\sigma,1} \right) K \sigma^2 + C_{\Delta,1} \frac{c\alpha L \Delta}{4m}. \end{aligned} \quad (42)$$

Divide both sides by  $\frac{\alpha cmK}{4}$  and utilize  $C_{f,1} \leq 1$ ,  $f(x^{(0)}) - f(\hat{x}^T) \leq \Delta$ ,  $m \geq c^{-2}n^2s_B^2$  and  $C_{\sigma,1} \leq \frac{73c\alpha L}{n} + \frac{384s_B^3s_{B^m}^2}{m^2c^2}$ ,  $T = mK$ , we have

$$\frac{1}{K} \sum_{k \in [m^*]} \mathbb{E}[\|\nabla f(\hat{x}^{(k)})\|^2] \leq \frac{\Delta}{c\alpha T} + \frac{100c\alpha L}{n}\sigma^2 + \frac{384s_B^3s_{B^m}^2}{m^2c^2}\sigma^2 + C_{\Delta,1}\frac{L\Delta}{mT}. \quad (43)$$

Inequality (43) holds when  $\alpha \leq \min\{\frac{1}{10cm\sqrt{s_Bs_{B^m}^2}}, \frac{1}{6L}\}$  and  $m$  is larger than some matrix-related constants.

To obtain a standard linear speedup result, we set

$$m = \lceil \max\{4c^{-1}s_B^{1.5}s_{B^m} \left(\frac{nT\sigma^2}{L\Delta}\right)^{0.25}, C_m\} \rceil,$$

$$\alpha = \min\left\{\frac{\sqrt{n\Delta}\sigma}{10c\sqrt{LT}}, \frac{1}{10cm\sqrt{s_Bs_{B^m}^2L}}, \frac{1}{6L}\right\},$$

giving that

$$\begin{aligned} \min_{t \in \{0,1,\dots,T-1\}} \mathbb{E}[\|\nabla f(\hat{x}^{(t)})\|^2] &\leq \frac{1}{K} \sum_{k \in [m^*]} \mathbb{E}[\|\nabla f(\hat{x}^{(k)})\|^2] \\ &\leq \frac{44\sigma\sqrt{L\Delta}}{\sqrt{nT}} + \frac{L\Delta(m^{-1}C_{\Delta,1} + 10m\sqrt{s_Bs_{B^m}^2} + c^{-1})}{T} \\ &= \frac{44\sigma\sqrt{L\Delta}}{\sqrt{nT}} + \mathcal{O}\left(\frac{L\Delta}{T}\right)^{\frac{3}{4}} + \mathcal{O}\left(\frac{L\Delta}{T}\right) \end{aligned}$$

## C Experiment Details

In this section, we supplement experiment setup details.

### C.1 Weight Matrix Design

We use the following procedure to generate a row/column-stochastic weight matrix. For a fixed number of nodes  $n$ , we begin by initializing a 0-1 adjacency matrix  $W$  as the identity matrix  $I$  to account for self-loops on each node. Subsequently, based on the specific network topology definition, we set  $W_{i,j} = 1$  if there is a directed edge from node  $i$  to node  $j$ . After constructing this initial 0-1 matrix  $W$ , we then randomly assign integer weights from 1 to 9 to all entries where  $W_{i,j} = 1$ . Finally, we perform either row normalization or column normalization on this weighted matrix to obtain a row-stochastic matrix  $A$  or a column-stochastic matrix  $B$ , respectively.

### C.2 Synthetic data

For experiments conducted on the synthetic dataset, the objective function is given by:

$$f(x) = \frac{1}{n} \sum_{i=1}^n f_i(x), \quad x \in \mathbb{R}^d, \quad (44)$$

where

$$f_i(x) = \underbrace{\frac{1}{L_i} \sum_{l=1}^{L_i} \ln(1 + \exp(-y_{i,l} h_{i,l}^\top x))}_{\text{Logistic Loss}} + \underbrace{\rho \sum_{j=1}^d \frac{[x]_j^2}{1 + [x]_j^2}}_{\text{Non-convex Regularization}}, \quad L_i = L_{\text{Local}}/n.$$

## Data Synthesis Process:

### 1. Global Data Generation:

- Generate optimal parameters:  $x_{\text{opt}} \sim \mathcal{N}(0, I_d)$
- Create global feature matrix  $H \in \mathbb{R}^{L_{\text{total}} \times d}$  with  $h_{l,j} \sim \mathcal{N}(0, 1)$
- Compute labels  $Y \in \mathbb{R}^{L_{\text{total}}}$  with  $y_l \in \{-1, +1\}$  via randomized thresholding:

$$y_l = \begin{cases} 1 & \text{if } 1/z_l > 1 + \exp(-h_l^\top x_{\text{opt}}) \\ -1 & \text{otherwise} \end{cases}, \quad z_l \sim \mathcal{U}(0, 1)$$

### 2. Data Distribution:

- Partition  $H$  and  $L$  across  $n$  nodes using:

$$H^{(i)} = H[iM : (i+1)M, :], \quad Y^{(i)} = Y[iM : (i+1)M], \quad M = L_{\text{total}}/n$$

where  $L_{\text{total}}$  must be divisible by  $n$

### 3. Local Initial Points:

$$x_i^* = x_{\text{opt}} + \varepsilon_i, \quad \varepsilon_i \sim \mathcal{N}(0, \sigma_h^2 I_d), \quad \sigma_h = 10$$

**Gradient Computation:** At each iteration, each node  $i$  independently computes its stochastic gradient by randomly sampling a minibatch of size  $B$  from its local dataset of size  $L_i = L_{\text{total}}/n$ . The gradient computation consists of two components:

$$\nabla f_{i,B}(x) = -\underbrace{\frac{1}{B} \sum_{b=1}^B \frac{y_{i,b} h_{i,b}}{1 + \exp(y_{i,b} h_{i,b}^\top x)}}_{\text{Logistic Loss Gradient}} + \underbrace{\rho \sum_{j=1}^d \frac{2[x]_j}{(1 + [x]_j^2)^2}}_{\text{Non-convex Regularization}}$$

where the minibatch  $\{h_{i,b}, y_{i,b}\}_{b=1}^B$  is drawn uniformly from the  $L_i$  local samples without replacement. Notice that the gradient on each node  $i$  is computed on the local parameter  $x_i \in \mathbb{R}^d$ .

### Implementation Details:

- Global dataset size  $L_{\text{total}} = 204800$ , batch size  $B = 200$
- Dimension  $d = 10$ , regularization  $\rho = 0.01$
- Node configurations:  $n \in \{4, 6, 8, 9, 12, 16, 18, 24, 25\}$ , and the least common multiple (LCM) is 3,600.



Notice that  $L_{\text{total}} = 1,440,000 = 3,600 \cdot 200 \cdot 2 = \text{LCM} \cdot B \cdot 2$ .

**Evaluation Metric:** We track  $\|n^{-1} \mathbf{1}^\top \nabla f(\mathbf{x}^{(k)})\|$  as gradient norm, where

$$n^{-1} \mathbf{1}^\top \nabla f(\mathbf{x}^{(k)}) = \frac{1}{n} \sum_{i=1}^n \nabla f_{i,M}(\mathbf{x}_i^{(k)}), \quad M = L_{\text{Total}}/n.$$

The experimental results shown in our plots represent the average performance across 20 independent repetitions, where each trial is conducted with the fixed random seed = 42 for reproducibility.

### C.3 Neural Network Experiment

We first employ three-layer fully connected neural networks for MNIST classification.

**Data Distribution:** For each node  $k \in \{1, \dots, n\}$ , we sample a class proportion vector

$$\mathbf{q}^k = (q_{k,0}, q_{k,1}, \dots, q_{k,9}) \sim \text{Dirichlet}(\alpha \cdot \mathbf{1}^{10})$$

where  $\mathbf{1}^{10}$  is a 10-dimensional vector of ones. Each  $q_{k,c}$  represents the target proportion of samples from class  $c$  that node  $k$  should ideally hold. By definition of the Dirichlet distribution,  $q_{k,c} \geq 0, \forall c$  and  $\sum_{c=0}^9 q_{k,c} = 1, \forall k$ .

Denote  $N_{k,c}^{\text{target}} = q_{k,c} \cdot \frac{M}{n}$  as the target number of samples of class  $c$  to be assigned to node  $k$ . Ignoring the slight deviations caused by non-divisibility, the number of samples assigned to each node  $k$  is approximately  $60,000/n$ . Here we set  $\alpha = 0.9$  to get the heterogeneous data and the Figure 5 shows the distribution of samples with 16 nodes. The Figure 2 shows that the Push Pull achieves linear speedup on synthetic data.

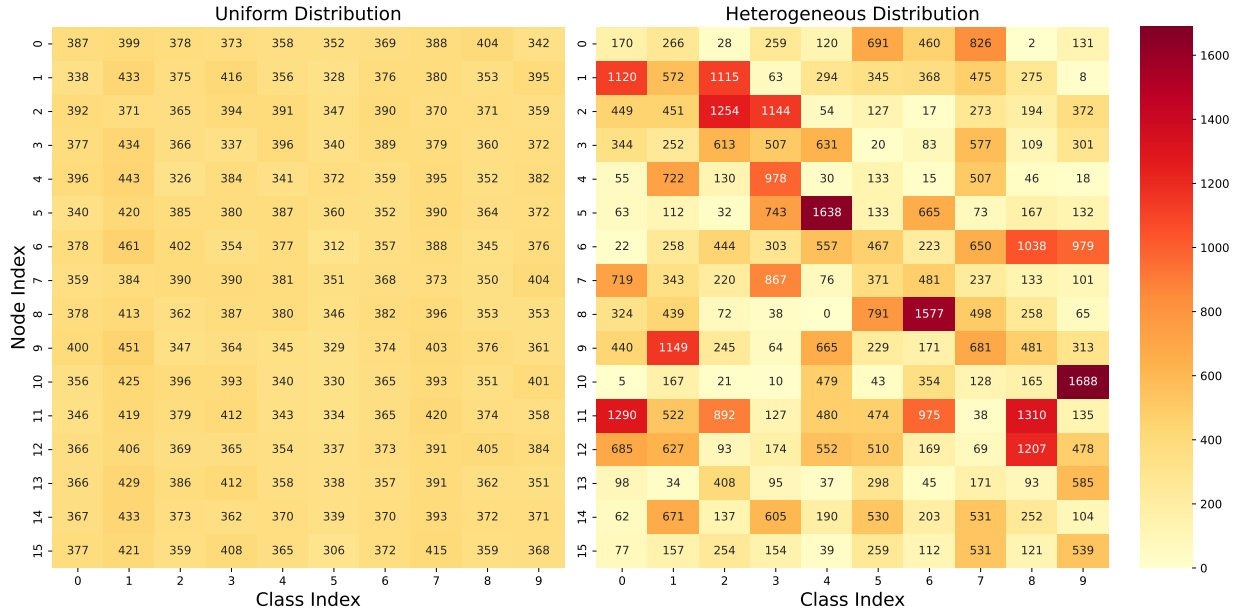


Figure 5: Comparison of uniform (left) and heterogeneous (right) data distributions across 16 nodes ( $\alpha = 0.9$ ).

**Evaluation Metric:** After each batch computation, we first average the gradients obtained from the  $n$  neural networks. Then we compute the norm of this averaged gradient. This norm is subsequently normalized

by the number of parameters  $\mathbf{P}$  of a single neural network. In our experiments,  $\mathbf{P} = 1,863,690$ .

$$\left\| \frac{1}{n} \sum_{i=1}^n \mathbf{g}_{i,B_{ij}} \right\|_2 / \sqrt{\mathbf{P}}, \text{ the gradient } \mathbf{g}_{i,B_i} \text{ is computed on the } j\text{-th batch of node } i \quad (45)$$

The Figure 3 shows that the Push Pull achieves linear speedup on both directed and undirected topologies.

Finally, we trained Resnet18 models on the CIFAR10 dataset to evaluate the performance of our PUSH-PULL method on a benchmark computer vision task. This involved conducting training across different numbers of nodes ( $n > 1$ ) utilizing the three previously described network topologies: directed exponential, grid graphs, and undirected random graphs. The performance was compared to single-node training ( $n = 1$ ) without distributed optimization. (see Figure 4).

#### Implementation Details:

- Learning rate  $lr = 0.005$  on each topology and each number of node.
- Batch size  $bs = 128$  on each topology and each number of node.